

A DYNAMICAL STUDY OF GALAXIES IN THE HICKSON COMPACT GROUPS

SHINGO NISHIURA^{1,2}, MASASHI SHIMADA^{1,2,3}, YOUICHI OHYAMA^{2,4}, TAKASHI
MURAYAMA^{1,2}, AND YOSHIAKI TANIGUCHI^{1,2}

¹Astronomical Institute, Graduate School of Science, Tohoku University, Aramaki, Aoba,
Sendai 980-8578, Japan

²Visiting astronomer of Okayama Astrophysical Observatory, National Astronomical
Observatory of Japan

³PENTAX

⁴National Astronomical Observatory of Japan, 2-21-1 Osawa, Mitaka, Tokyo 181-8588,
Japan

Received _____; accepted _____

ABSTRACT

In order to investigate dynamical properties of spiral galaxies in the Hickson compact groups (HCGs), we present rotation curves of 30 galaxies in 20 HCGs. We found as follows. 1) There is not significant relation between dynamical peculiarity and morphological peculiarity in HCG spirals. 2) There is no significant relation between the dynamical properties and the frequency distribution of nuclear activities in HCG spirals. 3) There are no significant correlations between the dynamical properties of HCG spirals and any group properties (i.e., the size, the velocity dispersion, the galaxy number density, and the crossing time). 4) Asymmetric and peculiar rotation curves are more frequently seen in the HCG spirals than in field spirals and in cluster ones. However, this tendency is more obviously seen in late-type HCG spirals. These results suggest that the dynamical properties of HCG spirals do not strongly correlate with the morphology, the nuclear activity, and the group properties. Our results also suggest that more frequent galaxy collisions occur in the HCGs than in the field and in the clusters.

Subject headings: galaxies: clustering - galaxies: interactions - galaxies: internal motions

1. INTRODUCTION

Dynamical properties of a galaxy are basically governed by both the mass and angular-momentum distributions in the galaxy. Since such dynamical properties are deeply related to the formation and evolution of galaxies, many dynamical studies have been done for various kinds of galaxies (e.g., Rubin et al. 1985; see for recent papers, Rubin, Waterman, & Kenney 1999; Sofue et al. 1999). Dynamical properties also provide important information on the interaction between galaxies (Keel 1993, 1996; Chengalur et al. 1994; Márquez & Moles 1996; Barton, Bromley, & Gellar 1999) and on the galaxy environment such as clusters of galaxies (Rubin et al. 1988, 1999; Whitmore et al. 1988).

In addition to the central region of clusters of galaxies, compact groups (CGs) of galaxies are also useful laboratories to investigate violent interactions between/among galaxies because they are small and isolated systems whose galaxy number densities are comparable to those of the center of cluster of galaxies; e.g., $\sim 10^{4-6}$ galaxies Mpc^{-3} (Shakhbazyan 1973; Rose 1977; Hickson 1982). Among such CGs, the Hickson compact groups (HCGs) of galaxies have been studied extensively (Hickson 1982, 1993). Many galaxies in the HCGs show peculiar morphologies such as tidal tails, tidal bridges, distorted isophotes, shell structures, and so on (Mendes de Oliveira & Hickson 1994). It is also known that a number of early-type galaxies in the HCGs have unusually blue colors (Zepf et al. 1991; Moles et al. 1994). These observational results suggest that galaxies in the HCGs have experienced frequent dynamical interactions. Indeed, Rubin et al. (1991) showed that rotation curves of many spiral galaxies in HCGs appear abnormal.

In order to investigate the effect of dynamical interactions in the CG environment, we newly conducted an optical spectroscopy program of HCG galaxies (Shimada et al. 2000: Paper I). This paper presents results of statistical studies with rotation curve properties of HCG spirals. We describe our observation and the data reduction in section 2. Making

rotation curve, estimation of rotation curve asymmetry, classifying rotation curve shapes are described in section 3. In section 4 we compare the rotation curve properties of the HCG spiral galaxies with the optical morphologies, nuclear activities, group properties (the group size, the velocity dispersion, the galaxy number density, and the crossing time). We compare the rotation curve properties between the HCG spirals and field ones in section 5 and clusters ones in section 6. In section 7 we discuss our results.

We adopt a Hubble constant $H_0 = 100 \text{ km s}^{-1} \text{ Mpc}^{-1}$ and a deceleration parameter $q_0 = 0$ throughout this paper.

2. OBSERVATIONS

We have obtained optical long-slit spectra along major-axis of 30 galaxies (mostly disk galaxies) in 20 HCGs. The sample galaxies were selected randomly from the HCG catalog (Hickson 1993). The optical spectroscopy was made using the new Cassegrain spectrograph with an SITe 512×512 CCD camera attached to the 188 cm telescope at the Okayama Astrophysical Observatory (OAO) during a period between 1996 February and 1997 January. A journal of the observations is given in Table 1. Basic data of the observed galaxies from Hickson (1993) are summarized in Table 2. As for the morphology type, we preferentially adopted the Hubble Type taken from de Vaucouleurs et al. (1991, hereafter RC3). For galaxies whose Hubble type are uncertain in RC3, we adopted the Hubble type taken from Hickson (1993).

A long (5 arcmin) slit with a width of 1.8 arcsec was used and put on each target galaxy with a position angle of the major axis. The 600 grooves mm^{-1} grating was used to cover $6300 - 7050 \text{ \AA}$ region with the spectral resolution of 3.4 \AA ($\simeq 157 \text{ km s}^{-1}$ in velocity at 6500 \AA). Two-pixel binning was made of the CCD along the slit and thus the spatial

resolution was 1.75 arcsec per element. The typical seeing during the runs was 2 arcsec.

The data were analyzed using IRAF¹. We also used a special data reduction package, SNGRED (Kosugi et al. 1995), developed for OAO new Cassegrain spectrograph data. The reduction was made with a standard procedure; bias subtraction, flat fielding with the data of the dome flats, and cosmic ray removal. Flux calibration was obtained using standard stars available in IRAF.

3. RESULTS

3.1. Major-axis Velocity Curves

We use the H α emission line to construct a heliocentric velocity curve as a function of the radial distance (r) from the nucleus for each galaxy; i.e., $V_{\text{obs}}(r) = c[\lambda_{\text{obs}}(r)/\lambda_0 - 1]$ where $\lambda_{\text{obs}}(r)$ and λ_0 are the measured and the rest-frame wavelengths of H α , respectively. For each galaxy, we derive the rotation velocity curve correcting for the inclination effect; i.e., $V(r) = [V_{\text{obs}}(r) - V_{\odot}]/[(1 + V_{\odot}/c) \sin i]$ where V_{\odot} is the heliocentric velocity of the galaxy center, c is the light velocity, and i is the inclination angle of the galaxy ($i = 0^{\circ}$ corresponds to the face-on view). Following Rubin et al. (1982), we estimate the inclination angle using a relation of $\sin i = 1.042^{0.5}(1 - 10^{-2x})^{0.5}$ where $x = \log(R_{\text{major}}/R_{\text{minor}})$; R_{major} and R_{minor} are the semimajor and semiminor axis of the isophote at 25 mag arcsec⁻² in the B band, respectively (Hickson 1993). The adopted values of $\sin i$ are given in Table 2. Distances from galactic nucleus r , rotation velocities $V(r)$ and their 1 σ fitting error $dV(r)$ are given in Table 15 (Appendix). In Figure 1, we show the rotation velocity curves as a

¹Image Reduction and Analysis Facility (IRAF) is distributed by the National Optical Astronomy Observatories, which are operated by the Association of Universities for Research in Astronomy, Inc., under cooperative agreement with the National Science Foundation.

function of distance from the galactic nucleus in units of arcsec for the observed galaxies.

3.2. Asymmetry of the Rotation Curve

It is known that galaxy collisions disturb the rotation curves of galaxies. The kinematical effect due to the tidal disturbance is often different between the side facing to the colliding partner and the opposite side and thus the rotation curve tends to show an asymmetrical property (Barton et al. 1999 and references therein). Therefore, it is interesting to investigate the asymmetry of the rotation curve. In order to quantify the asymmetry of the rotation curve, we define an asymmetry parameter A ,

$$A \equiv \left[\frac{1}{N} \sum_j^N \left(\frac{[V(r_j) - V(-r_j)]}{[V(r_j) + V(-r_j)]} \right)^2 \right]^{1/2}, \quad (1)$$

where j is the bin number along the major axes and N is the total bin number. Here we use the data between $r = 0.2R_{25}$ and $r = 0.5R_{25}$, where R_{25} is length of the radius of the isophote at 25 mag arcsec⁻² in the B band. The reason for this is as follows. The minimum radius, $0.2R_{25}$, is adopted to exclude the data in the central region of galaxies where the tidal disturbance is expected to be negligibly small; i.e., if we include the data with $r < 0.2R_{25}$, the difference of the asymmetry parameter among the galaxies could be less pronounced. On the other hand, the maximum radius, $0.5R_{25}$, is adopted to cover the observed rotation curves for most of the galaxies studied here. According to the definition of A , galaxies with higher asymmetric rotation curves tend to have larger values of A . The results are given in Table 3. We cannot estimate A for six spirals (HCG 37b, 47a, 61c, 87a, 92c, and 96a) because of the small data points in their rotation curves.

3.3. Shape of the Rotation Curves

As shown in Figure 1, the observed velocity curves show various shapes. However, we simply adopt following three types of shapes; 1) Type “f”: the rotation velocity monotonically rises near the center and tend to be almost flat at $r/R_{25} \leq 1$; note that most ordinary spiral galaxies have this type of rotation curves (e.g., Rubin et al. 1985), 2) Type “fp”: the rotation curve appears almost flat but some dips and/or bumps are seen, 3) Type “p”: the rotation curve shows a significantly peculiar shape. Rotation curves with a sinusoidal shape or a linearly-rising shape are included in this type. The results of our classification are given in Table 3. Note that rotation curves of two galaxies (HCG 37b, and 92c) cannot be classified because there are only few data points.

4. THE ROTATION CURVE PROPERTIES OF HCG GALAXIES

4.1. Enlarged HCG Sample

Among the 30 galaxies observed by us, two galaxies are redshift-discordant galaxies in the HCGs (HCG 73a and 92a). One of remaining 28 galaxies is classified as an S0 in RC3 (HCG 87a). Therefore, our HCG sample contains 27 spiral galaxies. In order to enlarge the sample, we add HCG galaxies observed by Rubin et al. (1991) (see Table 4). Their sample contains 34 spiral galaxies. Excluding two no-available galaxies (HCG 10a and 37c) of which rotation curve data were not shown, two redshift-discordant galaxies (HCG 31d and 78a), and five S0 galaxies classified in RC3 (HCG 16c, 16d, 23a, 34b, and 57e), we obtained the rotation curve data of the 25 HCG spirals from Rubin et al. (1991). For these 25 HCG spiral galaxies, we estimate the asymmetry parameter and classify the rotation curve shape with the same method for our HCG data. The results are also given in Table 4. Twelve of these 25 spiral galaxies are commonly observed (HCG 31a, 31b, 31c, 37b, 40c,

44a, 44b, 44d, 79d, 88a, 88c, and 89a). The A values of these twelve spirals are adopted the averaged A . Finally, we obtain an enlarged HCG sample which contains 40 spiral galaxies. Hereafter, we discuss the rotation curves of HCG spirals with the enlarged HCG spiral sample containing 40 spirals.

4.2. Rotation Curve Properties versus Morphologies of Host Galaxies

Mendes de Oliveira & Hickson (1994) showed that about a half of galaxies in HCGs have peculiar morphologies such as tidal tails, tidal debris, distorted isophotes, and so on, indicating evidence for galaxy collisions. On the other hand, Rubin et al. (1991) found that there is a loose correlation between peculiarity of rotation curve and peculiarity of morphology. In Table 5, we classified our HCGs spiral galaxies into two categories based on the optical morphology from Mendes de Oliveira & Hickson (1994) and RC3. The spiral galaxies with or without optical peculiar morphologies are listed in Table 5. We compare the shape of rotation curves with the optical morphologies of host galaxies. The result is shown in Table 6. Although it is generally expected that spiral galaxies with normal rotation curve have normal morphology and those with peculiar rotation curve have peculiar morphology, there are normal morphology galaxies with peculiar kinematics, and peculiar morphology galaxies with normal kinematics. We adopted the null hypothesis that distribution for the HCG spiral galaxies with peculiar morphology is the same as that for with normal morphology and apply the χ^2 test. The result is shown in Table 6. We obtained a probability, $P(\chi^2) = 0.818$. We find that there is no significantly statistical difference between the HCGs spiral galaxies with peculiar morphology and that with normal morphology.

4.3. Rotation Curve Properties versus Nuclear Activities

It has often been considered that frequent galaxy collisions trigger some nuclear activities (active galactic nuclei or intense star formation) in HCG member galaxies. Therefore, it is interesting to compare the kinematical properties in the member galaxies with the nuclear activity.

Using observed flux ratio of [NII] to $H\alpha$, we classify the activities of galaxies into active galactic nuclei (AGN) and HII nucleus galaxies (HII); galaxies with $f([\text{NII}])/f(H\alpha) \geq 0.6$ are classified into AGN, and those with $f([\text{NII}])/f(H\alpha) < 0.6$ are classified into HII (Ho et al. 1997). The $f([\text{NII}])/f(H\alpha)$ ratio and the activity type for each galaxy are listed in Table 5. In Figure 2, we compare the distributions of the asymmetry parameter A between AGNs and HII nuclei. We apply the Kolmogorov-Smirnov (KS) test (e.g. Press et al. 1988). The null hypothesis is that the distributions of A of both the AGN and the HII nuclei come from the same underlying population. We obtain a KS probability, 0.947. This indicates that there is no difference in the distribution of the asymmetry parameter between the HCG AGN and the HCG HII nuclei. In Figure 3, we show diagrams of [NII]/ $H\alpha$ ratio against the asymmetry parameter A . The left panel is the diagram for the case of early-type (S0/a-Sbc) and late-type (Sc and later) spirals and the right panel is the one for the case of “f” rotation curves, “fp” ones, and “p” ones. We adopt the null hypothesis that the asymmetry parameter A is not correlated with [NII]/ $H\alpha$ ratio and apply the Spearman-rank statistical test for all the case shown in Figure 3. A summary of the statistical tests is given in Table 7. There is no correlation between the A and [NII]/ $H\alpha$ ratio in the HCG spirals.

4.4. Rotation Curve Properties versus Group Properties

Rubin et al. (1991) mentioned that there appears no correlation between normal or abnormal rotation curves and the velocity dispersion of the group. In order to confirm this, we investigate correlations between dynamics and other properties of group. From previous studies by Hickson et al. (1988, 1992), the group size, the velocity dispersion, the galaxy number density, and the crossing time are listed in Table 5 for each HCG galaxy. Figure 4(a)-(d) show relations between the asymmetry parameter A and the group size (Hickson et al. 1992), the velocity dispersion (Hickson et al. 1992), the galaxy number density (Hickson et al. 1988), and the crossing time (Hickson et al. 1992) for case of early-type (S0/a-Sbc), late-type (Sc and later), “f” rotation curves, “fp” ones, and “p” ones. We adopt the null hypothesis that the asymmetry parameter A is not correlated with each group property and apply the Spearman-rank statistical test for all the correlations shown in Figure 4(a)-(d). A summary of the statistical tests is given in Table 8. Although the probability between A and group velocity dispersion for “f” rotation curves is 4.81×10^{-3} , the three σ confidence level is 1.3×10^{-3} . Therefore, for any cases, it is found that there is no correlation between the asymmetry parameter A and the group properties.

5. COMPARISON OF ROTATION CURVES BETWEEN HCG GALAXIES AND FIELD GALAXIES

5.1. The Field Sample

In order to investigate how the dynamical properties of HCG galaxies are different from those of isolated galaxies, we need a reference sample of field galaxies. Rubin et al. (1980, 1982, 1985) published rotation curves for 60 spiral galaxies (16 Sa, 23 Sb, and 21 Sc galaxies). Excluding two Virgo spiral galaxies (NGC 4321 and NGC 4419) and two galaxies

in groups (NGC 1353 and NGC 4448), we adopt 56 spiral galaxies (15 Sa, 21 Sb, and 20 Sc) as a field galaxy sample. The basic data of these field galaxies are summarized in Table 9.

Unfortunately, Rubin et al. (1980, 1982, 1985) show only average rotation velocity $V(|r|)$ which is the mean of velocities within the radial bins of both r and $-r$, and 1σ error of the mean, $dV(|r|)$. It is hard to know how many data points either r or $-r$ contains and to estimate $V(r)$ and $V(-r)$. Therefore, we simply assume that there is only one velocity data point in each bin of r and $-r$. Making $V(r)$ and $V(-r)$ that here we reconstruct with $V(|r|)$ and $dV(|r|)$ of Rubin et al. (1980, 1982, 1985) under such assumption, one finds that the rotation velocity at distance r is $V(r) = V(|r|) + dV(|r|)/\sqrt{2}$ and that the rotation velocity at distance $-r$ is $V(-r) = V(|r|) - dV(|r|)/\sqrt{2}$. In this case we can define the asymmetry parameter A as,

$$A \equiv \frac{1}{\sqrt{2}} \left[\frac{1}{N} \sum_j \left(\frac{dV(|r_j|)}{V(|r_j|)} \right)^2 \right]^{1/2}. \quad (2)$$

The meaning of j and N are the same as those for the equation (1). Note that the asymmetry parameters A for field spirals are all upper limits according to the above definition.

We also classify the shape of rotation curves for field spiral galaxies. The asymmetry parameter A and the shape of the rotation curves for the field spiral galaxies are listed in Table 9.

5.2. Comparison of the Rotation Velocity between the HCG Spiral Galaxies and the Field Spiral Galaxies

In Figure 5, we show the rotation curves of our HCGs spiral galaxies as a function of distance from galactic nucleus in units of R_{25} . We also show expected rotation curves of the field galaxies calculated from synthetic rotation curves in Rubin et al. (1985). The rotation

curves of the HCG spiral galaxies are different from those of the field spiral galaxies. Many spiral galaxies in HCGs have peculiar rotation curves.

By numerical simulations, Barton et al. (1999) found that galaxy collision caused rising rotation curve. Some HCG spirals have such a rising rotation curve (e.g. HCG 61c and 88a). There are also spiral galaxies with higher rotation velocities (e.g. HCG 40c) and those with lower rotation velocities (e.g. HCG 88b and 88d) with respect to the field spirals with both the same Hubble type and the same luminosity.

Rubin et al. (1991) show that the HCG spirals tend to have lower rotation velocity with respect to the field ones. For some HCG spirals, we found the same tendency. However, it is difficult to determine intrinsic inclination angles i of HCG spirals showing peculiar morphologies. Although we estimated the inclination angles i of the HCG spirals, there is an uncertainty of i . Most of the rotation curves of HCG spirals are too peculiar to discuss the mass distribution in the galaxies.

5.3. Comparison of the Asymmetry Parameter between the HCG Spiral Galaxies and the Field Spiral Galaxies

We compare the frequency distributions of A between the HCGs and the field spiral galaxies in Figure 6. The comparison is carried out for the case of all Hubble type, S0/a – Sbc type, and Sc and later type galaxies. We include two field spiral galaxies with $A = 0$ into the smallest bin (NGC 2608 and IC 724). We find that A values of the HCG spirals are generally larger than those of the field spirals for all the morphological types. In particular, we mention that the maximum value of A of the field spirals is 0.06 (NGC 3054 and NGC 7171) while 18 HCGs spirals (53%) have $A > 1.0$.

We apply the KS test. The null hypothesis is that the observed distributions of A of

both the HCG galaxies and the field ones come from the same underlying population. We obtain KS possibilities (see Table 10); 1.15×10^{-11} for all the galaxies, 1.76×10^{-6} for S0/a – Sbc galaxies, and 7.40×10^{-7} for Sc and later-type spiral galaxies. Therefore, we conclude that the HCG galaxies tend to have asymmetrical rotation curves with respect to the field galaxies. This is consistent with the result of Rubin et al. (1991).

For the HCGs spirals, we find that the late-type (Sc and later) spirals have larger A than the early-type (S0/a – Sbc) ones. Applying the KS test, we obtain a probability of 2.32×10^{-3} between early-type HCG spirals and late-type HCG spirals while 0.792 for a comparison for that between early-type spirals in the field and late-type spirals in the field (see Table 10). Therefore, it is suggested that the HCG late-type spirals tend to have more asymmetrical rotation curves with respect to the HCG early-type ones.

5.4. Comparison of the Rotation Curve Shape between the HCG Spiral Galaxies and the Field Spiral Galaxies

We compare the rotation curve shapes between the HCG galaxies and the field ones. In Figure 7 we compare the frequency distributions of rotation curve shapes between the HCGs spirals and the field ones for all galaxies, early-type spirals, and late-type spirals. We adopt the null hypothesis that the distribution for the HCGs spirals is the same as that for the field ones and apply the χ^2 test. The results are given in Table 11. We find that there are significant statistical differences between the HCGs spirals and the field ones.

Among the 39 HCG galaxies, 33 ($\approx 85\%$) galaxies have either “fp” or “p” rotation curves. It is remarkable that almost all the HCG late-type spirals ($\approx 93\%$) have “p” rotation curves. On the contrary, only 42% of the HCG early-type spirals have “p” rotation curves and 21% of the HCG early-type spirals have “f” rotation curves.

The probability of the χ^2 test between the early-type field spirals and late-type field spirals is 0.673, while that between the early-type HCG spirals and the late-type HCG spirals is 4.44×10^{-3} . Although the latter probability suggests a marginally significant difference, a larger sample will be necessary to confirm it.

6. COMPARISON OF ROTATION CURVES BETWEEN HCG GALAXIES AND CLUSTER GALAXIES

6.1. The Cluster Sample

As we previously mentioned, the local galaxy number density of HCGs is comparable to that of cluster centers. Therefore it is interesting to compare the dynamical properties of the HCG spiral galaxies with those of cluster spiral galaxies. We use a sample of cluster spiral galaxies taken from Amram et al. (1992, 1994, and 1995) who published rotation curves of 41 spiral galaxies in eight clusters. The basic data of these cluster galaxies are summarized in Table 12. Their morphological types are taken from RC3 if available (32 galaxies). For the remaining nine spiral galaxies without RC3, we adopt the morphological types taken from Bell & Whitmore (1989), Amram et al. (1995), and Gavazzi & Boselli (1996).

Using the equation (1), we calculated the asymmetry parameter A of the cluster spiral galaxies. We also classified the shape of the rotation curves for them. The results are also listed in Table 12.

6.2. Comparison of the Asymmetry Parameter between the HCG Spiral Galaxies and the Cluster Spiral Galaxies

In Figure 6, we compare the frequency distribution of the asymmetry parameter A between the HCG spiral galaxies and the cluster ones. The comparison is carried out for the case of all Hubble types, S0/a – Sbc type, and Sc and later type galaxies. The null hypothesis is that the observed distributions of A of both HCG spirals and the cluster ones come from the same underlying population. Applying the KS test, we obtain the following KS probabilities (see Table 13); 6.64×10^{-4} for all the galaxies, 4.50×10^{-2} for the S0/a – Sbc spiral galaxies, and 8.48×10^{-4} for the Sc and later-type spiral galaxies. We find that the A values of HCG spiral galaxies tend to be larger than those of the cluster ones for all the case.

6.3. Comparison of the Rotation Curve Shape between the HCG Spiral Galaxies and the Cluster Spiral Galaxies

We show the frequency distribution of the rotation curve shape for the HCG, the field, and the cluster spirals in Figure 7. We compare the both distributions for the case of all Hubble type, S0/a-Sbc type, and Sc and later-type spirals. The null hypothesis is that the observed distributions of the rotation curve shape of both the HCG spirals and the cluster ones come from the same underlying population. Applying the χ^2 test, we obtain the following probabilities (see Table 14); 9.28×10^{-7} for all the galaxies, 3.84×10^{-3} for the S0/a-Sbc spirals, and 3.23×10^{-5} for the Sc and later-type spirals. These results suggest that the HCG spirals tend to show more peculiar shapes of rotation curve.

7. DISCUSSION

In this paper, we have investigated the asymmetry and the shape of the rotation curves of spiral galaxies in HCGs.

First, we investigated the relation between the morphological peculiarity and dynamical peculiarity of HCG spiral galaxies. We found that there is no statistical difference between them (Table 6), being consistent with the finding by Rubin et al. (1991). It is likely that the HCG spirals with both the morphological peculiarity and the dynamical peculiarity have experienced recent galaxy collisions. However, there are normal-morphology galaxies with peculiar dynamical properties and peculiar-morphology ones with normal dynamical properties. No correlation between the dynamical peculiarity and the morphological peculiarity suggests that the dynamical properties of the HCG spirals may be governed by galaxy collision parameters such as the difference of masses, and the orbital parameters. While the morphological peculiarities such as tidal tails and tidal bridges, and asymmetry come to be more clearly seen in outer regions of galaxies, the dynamical peculiarities probed by the $H\alpha$ line emission are observed in inner regions ($r < 0.5R_{25}$) of galaxies (see Figure 5). The morphological peculiarity can be more easily induced by galaxy collisions than the dynamical peculiarity. Thus, weak galaxy collisions could not perturb the galaxy rotation curves, although it is experienced that morphological deformation could be induced in outer parts of the galaxies. On the other hand, minor mergers could perturb the rotation curve in inner regions of galaxies without causing global morphological peculiarities.

Second, we investigated the relation between the properties of the rotation curves and the properties of the nuclear activity. Since it has often been suggested that the galaxy collisions trigger nuclear activities such as AGN and nuclear starburst phenomena

(Kennicutt & Keel 1984; Keel 1996), it is expected that such nuclear activities are more often observed in HCG galaxies. However, we found that there is no significantly statistical difference in the distribution of the asymmetry parameter A between the nuclear activities (Figure 2). We also found that there is no correlation between the asymmetry parameter A and $[\text{NII}]/\text{H}\alpha$ ratio (Figure 3). All these indicate that galaxy collisions do not always trigger the nuclear activity

Third, we investigated the relation between the dynamical properties of HCG spiral galaxies and the properties of the compact groups such as the group size, the velocity dispersion of member galaxies, the galaxy number density, and the crossing time (see Figure 4a-4d and Table 8). In compact groups with higher number densities and with smaller sizes, more frequent galaxy collision would occur and thus spiral galaxies in such groups would show more asymmetric rotation curves. However, we found that there are no significant correlations between the asymmetry parameter A and any group properties. There may be two alternative interpretations for this finding. 1) Many compact groups containing spiral galaxies are false groups; e.g., a pair of galaxies with a few field galaxies (Mamon 1986, 1992, 1994, 1995; Hernquist et al. 1995). 2) The projected size and the observed velocity dispersion of the compact groups are significantly different from the real (i.e., three-dimensional) ones. As mentioned in section 5.4, 85% of HCG spirals are peculiar and that 93 % of the late type HCG spirals are peculiar. This high rate of peculiarity seems inconsistent with the false group hypothesis. However, these two possibilities will be taken into account in future studies.

Finally, we compared the dynamical properties of spiral galaxies among the field, the clusters, and the HCGs. We found that the HCG spirals tend to have more asymmetric and more peculiar rotation curves with respect to the field and the cluster spirals (see Figure 6 and 7, Table 10, 11, 13, and 14). It is interesting to note that these are the significant

differences in the distributions of the A and the rotation curve morphologies between the HCG early-type spirals and the HCG late-type ones, although we found no such difference between the field early-type spirals and the field late-type ones. This may be attributed to the stabilization of a disk by a large bulge of early-type spirals (Mihos & Hernquist 1994; Velázquez & White 1999). Since a small bulge cannot stabilize the disk, late-type spirals are more sensitive to galaxy interactions than the early-type spirals and are expected to show the peculiar kinematical properties for a longer duration.

We are grateful to the staff of OAO for kind help of the observations. We would like to thank Daisuke Kawata and Tohru Nagao for useful comments and suggestions. TM is thankful for support from a Research Fellowship from the Japan Society for the Promotion of Science for Young Scientists. This work was partly supported by the Ministry of Education, Science, Culture, and Sports (Nos. 07044054, 10044052, and 10304013).

REFERENCES

- Adami, C., Marcelin, M., Amram, P., & Russeil, D. 1999, *A&A*, 349, 812
- Amram, P., Le Coarer, E., Marcelin, M., Balkowski, C., Sullivan, W. T., & Cayatte, V.
1992, *A&AS*, 94, 175
- Amram, P., Marcelin, M., Balkowski, C., Cayatte, V., Sullivan III, W. T., & Le Coarer, E.
1994, *A&AS*, 103, 5
- Amram, P., Boulesteix, J., Marcelin, M., Balkowski, C., Cayatte, V., & Sullivan III, W. T.
1995, *A&AS*, 113, 35
- Barton, E. J., Bromley, B. C., & Geller, M. J. 1999, *ApJ*, 511, 25
- Bell, M., & Whitmore, B. C. 1989, *ApJS*, 70, 139
- Chengalur, J. N., Salpeter, E. E., & Terzian, Y. 1994, *AJ*, 107, 1984
- de Carvalho, R. R., & Coziol, R. 1999, *ApJ*, in press (astro-ph/9901006)
- de Vaucouleurs, G., de Vaucouleurs, A., Corwin, H. G. Jr., Buta, R. J., Paturel, G.,
& Fouqué, P. 1991, *Third Reference Catalogue of Bright Galaxies* (Springer-
Verlag)(RC3)
- Dressler, A. 1980, *ApJ*, 236, 351
- Gavazzi, G., & Boselli, A. 1996, *Astrophys. Lett. & Comm.*, 35, 1
- Hernquist, L., Katz, N., & Weinberg, D. H. 1995, *ApJ*, 442, 57
- Hickson, P. 1982, *ApJ*, 255, 382
- Hickson, P. 1989, in *IAU Coll. 124, Paired and Interacting Galaxies*, ed. Sulentic, J. W.,
Keel, W. C. & Telesco, C. M. (NASA CP-3098) (Washington: GPO), 77
- Hickson, P. 1993, *Astrophys. Lett. & Comm.*, 29, 1
- Hickson, P., Kindl, E., & Huchra, J. P. 1988, *ApJ*, 331, 64

- Hickson, P., Mendes de Oliveira, C., Huchra, J. P., & Palumbo, G. G. C. 1992, *ApJ*, 399, 353
- Hickson, P., Menon, T. K., Palumbo, G. G. C., & Persic, M. 1989, *ApJ*, 341, 679
- Ho, L. C., Filippenko, A. V., & Sargent, W. L. W. 1997, *ApJS*, 112, 315
- Huchtmeier, W. K. 1997, *A&A*, 325, 473
- Iglesias-Páramo, J., & Vílchez, J. M. 1997a, *ApJ*, 479, 190
- Iglesias-Páramo, J., & Vílchez, J. M. 1997b, *ApJ*, 489, L13
- Iglesias-Páramo, J., & Vílchez, J. M. 1999, *ApJ*, 518, 94
- Keel, W. C. 1993, *AJ*, 106, 1771
- Keel, W. C. 1996, *ApJS*, 106, 27
- Kosugi, G., Ohtani, H., Sasaki, T., Koyano, H., Shimizu, Y., Yoshida, M., Sasaki, M., Aoki, K., & Baba, A. 1995, *PASP*, 107, 474
- Mamon, G. A., 1986, *ApJ*, 307, 426
- Mamon, G. A., 1992, *ApJ*, 401, 3
- Mamon, G. A., 1994, in *Clusters of Galaxies*, ed. Durret, F., Mazure, A., & Tran Thanh Van (Paris: Editions Frontieres), 297
- Mamon, G. A., 1995, in *Groups of Galaxies*, ASP Conf. Ser. 70, 83
- Márquez, I., & Moles, M. 1996, *A&AS*, 120, 1
- Mendes de Oliveira, C., & Hickson, P. 1994, *ApJ*, 427, 684
- Menon, T. K., 1992, *MNRAS*, 255, 41
- Menon, T. K., 1995, *MNRAS*, 274, 845
- Mihos, J. C., & Hernquist, L. 1994, *ApJ*, 431, 9

- Moles, M., Del Olmo, A., Perea, J., Masegosa, J., Márquez, I., & Costa, V. 1994, *A&A*, 285, 404
- Ponman, T. J., Bourner, P. D. J., Ebeling, H., & Böhringer, H. 1996, *MNRAS*, 283, 690
- Press, W. H., Teukolsky, S. A., Vetterling, W. T., & Flannery, B. P. 1988, in *NUMERICAL RECIPES in C*, (Cambridge University Press)
- Ribeiro, A. L. B., de Carvalho, R. R., Coziol, R., Capelato, H. V., & Zepf, S. E. 1996, *ApJ*, 463, 5
- Rose, J. A. 1977, *ApJ*, 211, 311
- Rubin, V. C., Burstein, D., Ford, W. K. Jr., & Thonnard, N. 1985, *ApJ*, 289, 81
- Rubin, V. C., Ford, W. K. Jr., & Thonnard, N. 1980, *ApJ*, 238, 471
- Rubin, V. C., Ford, W. K. Jr., Thonnard, N., & Burstein, D. 1982, *ApJ*, 261, 439
- Rubin, V. C., Hunter, D. A., & Ford, W. K. Jr. 1991, *ApJS*, 76, 153
- Rubin, V. C., Waterman, A. H., & Kenney, J. D. P. 1999, *AJ*, 118, 236
- Rubin, V. C., Whitmore, B. C., & Ford, W. K. Jr. 1988, *ApJ*, 333, 522
- Shakhbazyan, R. K. 1973, *Astrofiz*, 9, 495
- Shimada, M., Ohyama, Y., Nishiura, S., Murayama, T., & Taniguchi, Y. 2000, *AJ*, submitted
- Sofue, Y., Tutui, Y., Honma, M., Tomita, A., Takamiya, T., Koda, J., & Takeda, Y. 1999, *ApJ*, 523, 136
- Sulentic, J. W., & de Mello Rabaça, D. F. 1993, *ApJ*, 410, 520
- Taniguchi, Y., & Wada, K. 1996, *ApJ*, 469, 581
- Valluri, M., & Anupama, G. C., 1996, *AJ*, 112, 1390
- Velázquez, H., & White, S. D. M. 1999, *MNRAS*, 304, 254

Whitmore, B. C., Forbes, D. A., & Rubin, V. C. 1988, *ApJ*, 333, 542

Williams, B. A., & Rood, H. J. 1987, *ApJS*, 63, 265

Zepf, S. E., Whitmore, B. C., & Levison, H. F. 1991, *ApJ*, 383, 524

Fig. 1.— Major-axis velocities with respect to the systemic heliocentric velocity for 30 HCG galaxies as a function of projected nuclear distance.

Fig. 2.— Comparisons of frequency distributions of the logarithmic asymmetric parameter ($\log A$) between the AGN (upper panels) and HII nuclei (lower panels).

Fig. 3.— The relations between the logarithmic asymmetry parameter A and the $[\text{NII}]/\text{H}\alpha$ ratio. The filled circles and open circles indicate the early-type (S0/a-Sbc) and the late-type (Sc and later) HCG spiral galaxies. The open squares, filled squares, and crosses indicate the “f”, “fp”, and “p” rotation curves, respectively.

Fig. 4.— The relations between the logarithmic asymmetry parameter A and a) the size, b) the velocity dispersion, c) galaxy number density, and d) crossing time of group. The filled circles and open circles indicate the early-type (S0/a-Sbc) and the late-type (Sc and later) HCG spiral galaxies. The open squares, filled squares, and crosses indicate the “f”, “fp”, and “p” rotation curves, respectively.

Fig. 5.— Major-axis velocities with respect to the systemic heliocentric velocity for 30 HCG galaxies as a function of nuclear distance in the unit of R_{25} . The open circles and filled circles indicate approaching side and going away side. The middle line of three indicates expected rotation curves of the field spiral galaxies with similar Hubble type and luminosity calculated from synthetic rotation curves in Rubin et al. (1985). The top and bottom line of three are expected rotation curves of the field spiral galaxies with similar Hubble type and one magnitude brighter and fainter luminosity.

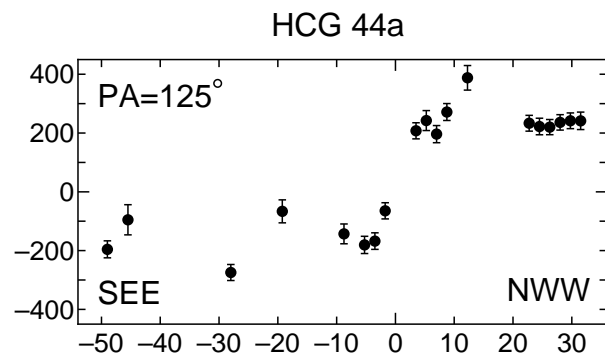
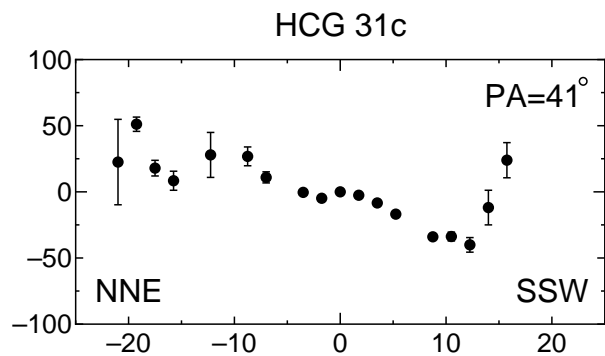
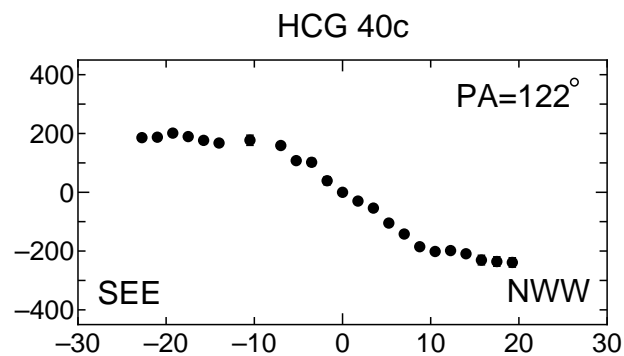
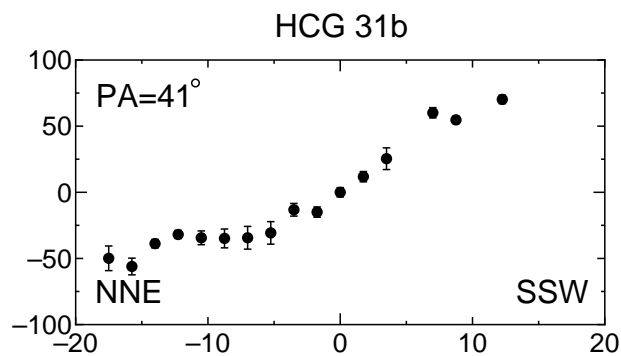
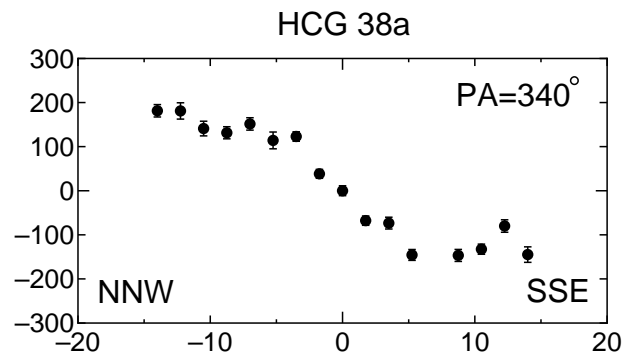
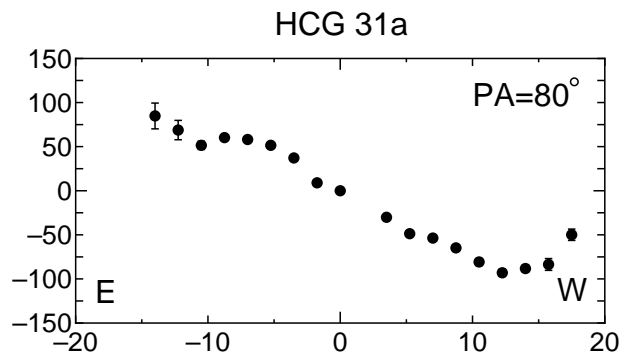
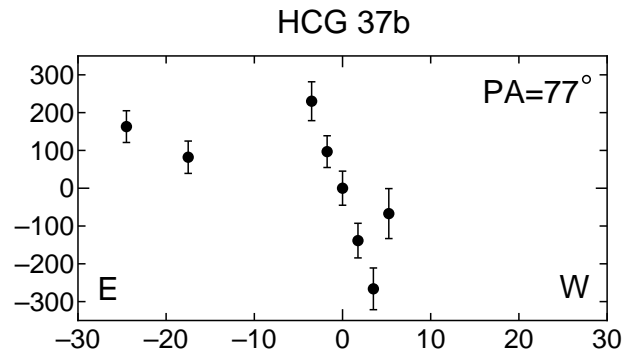
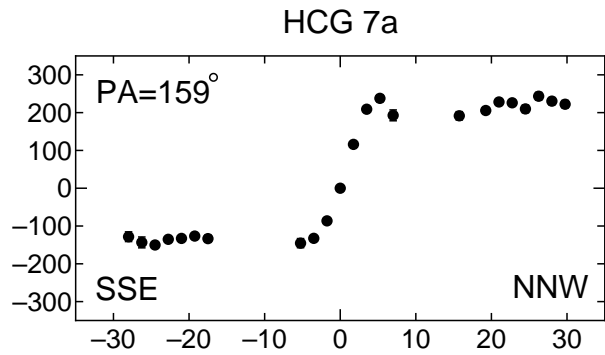
Fig. 6.— Comparisons of frequency distributions of the logarithmic asymmetric parameter ($\log A$) between the HCG spirals (upper three panels), the field ones (middle three panels), and the cluster spirals (lower three panels), for all Hubble type, early-type (S0/a-Sbc), and late-type (Sc and later).

Fig. 7.— Comparison of frequency distributions of the rotation curve shapes between the HCG spirals (upper panel), the field ones (middle panel), and the cluster ones (lower panel) for all Hubble type, early-type (S0/a-Sbc), and late-type (Sc and later).

A. Velocities for spirals in Hickson compact groups

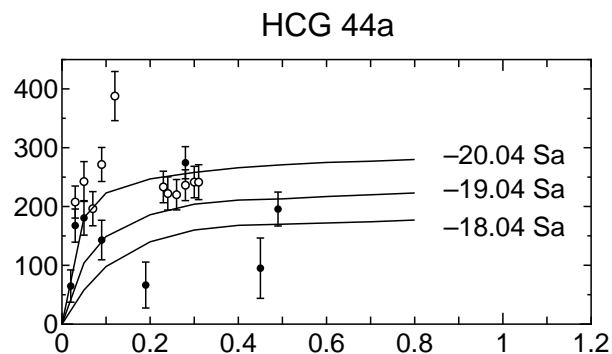
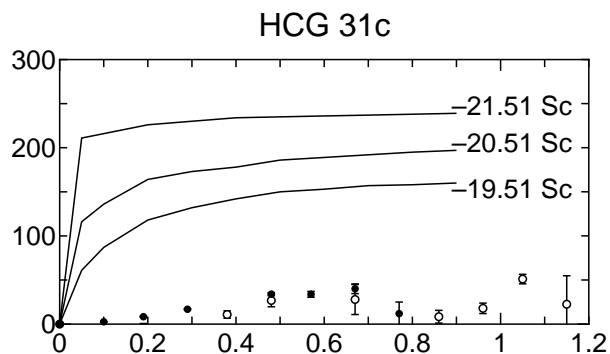
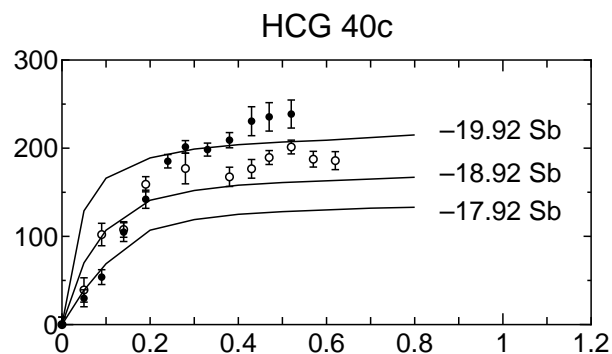
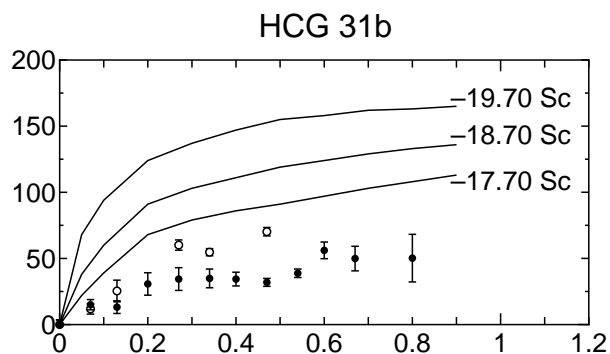
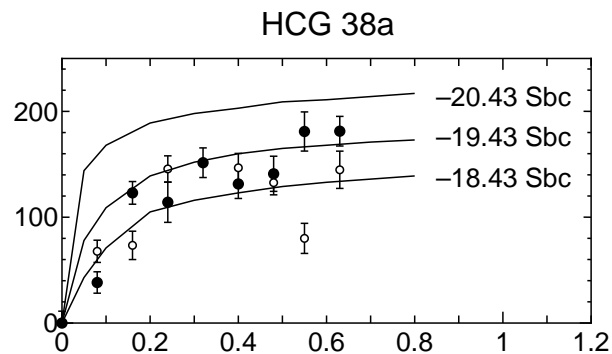
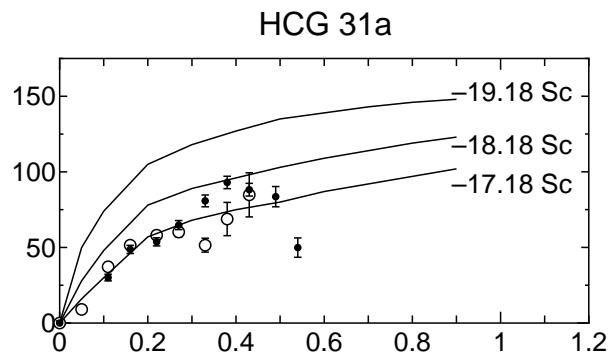
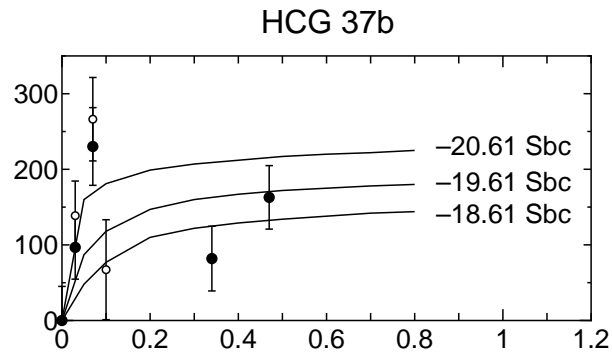
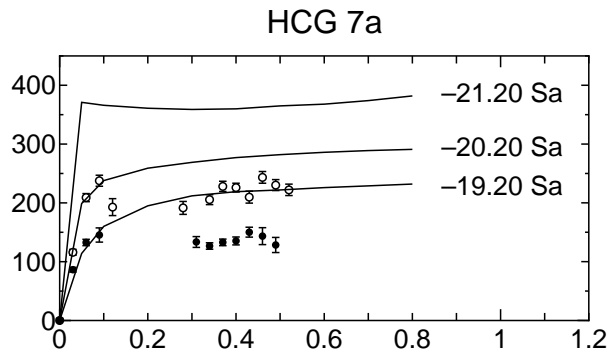
Table 15 lists the distances from galactic nucleus r in units of arcsec and of R_{25} , the rotation velocities $V(r)$ at r , and their 1σ errors $dV(r)$ for each observed HCG spirals.

ROTATION VELOCITY (km s^{-1})



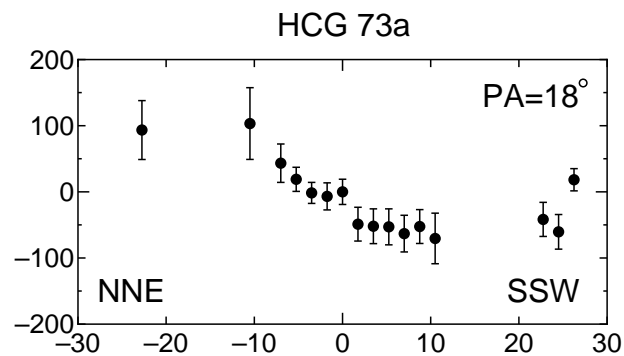
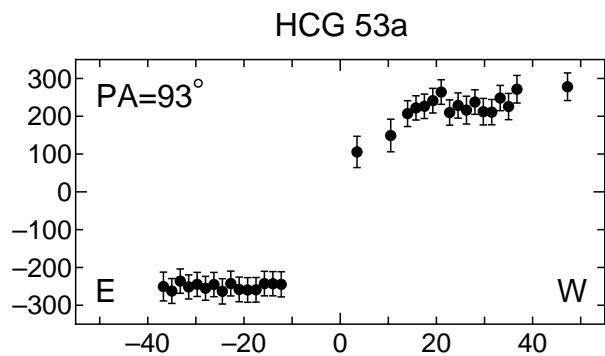
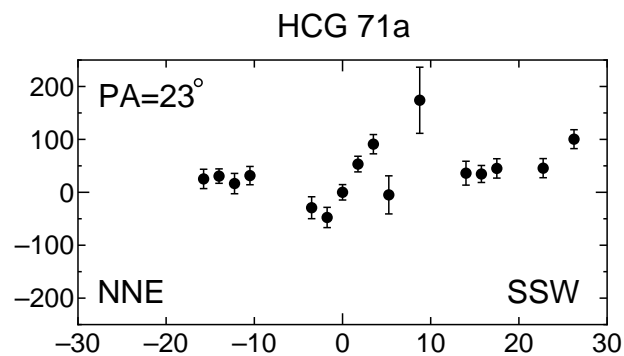
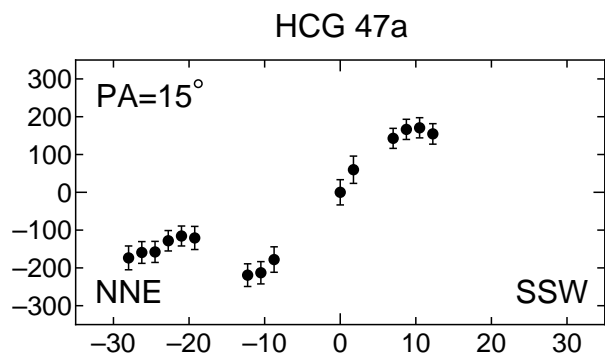
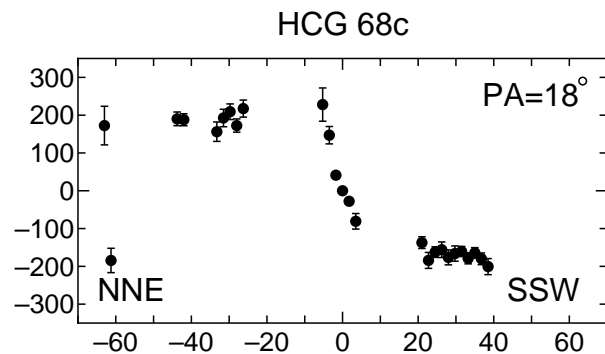
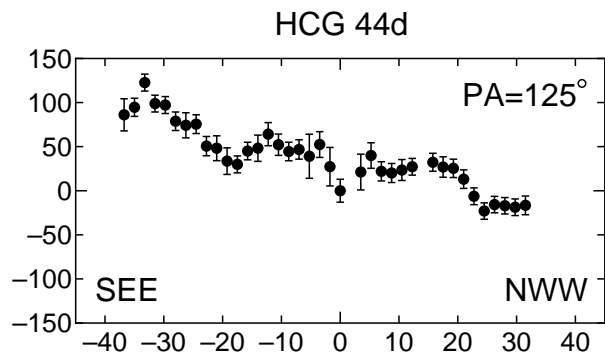
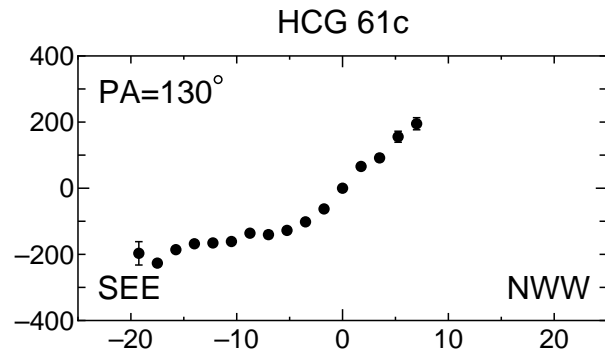
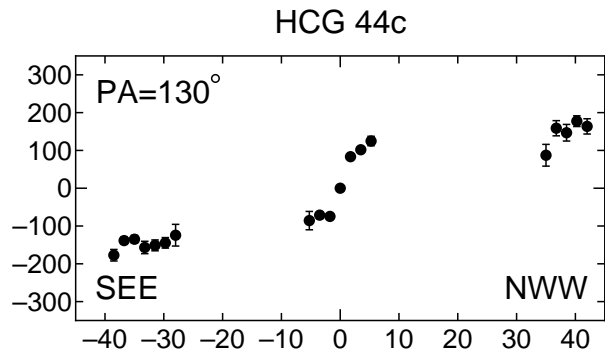
DISTANCE FROM NUCLEUS (arcsec)

ROTATION VELOCITY (km s^{-1})

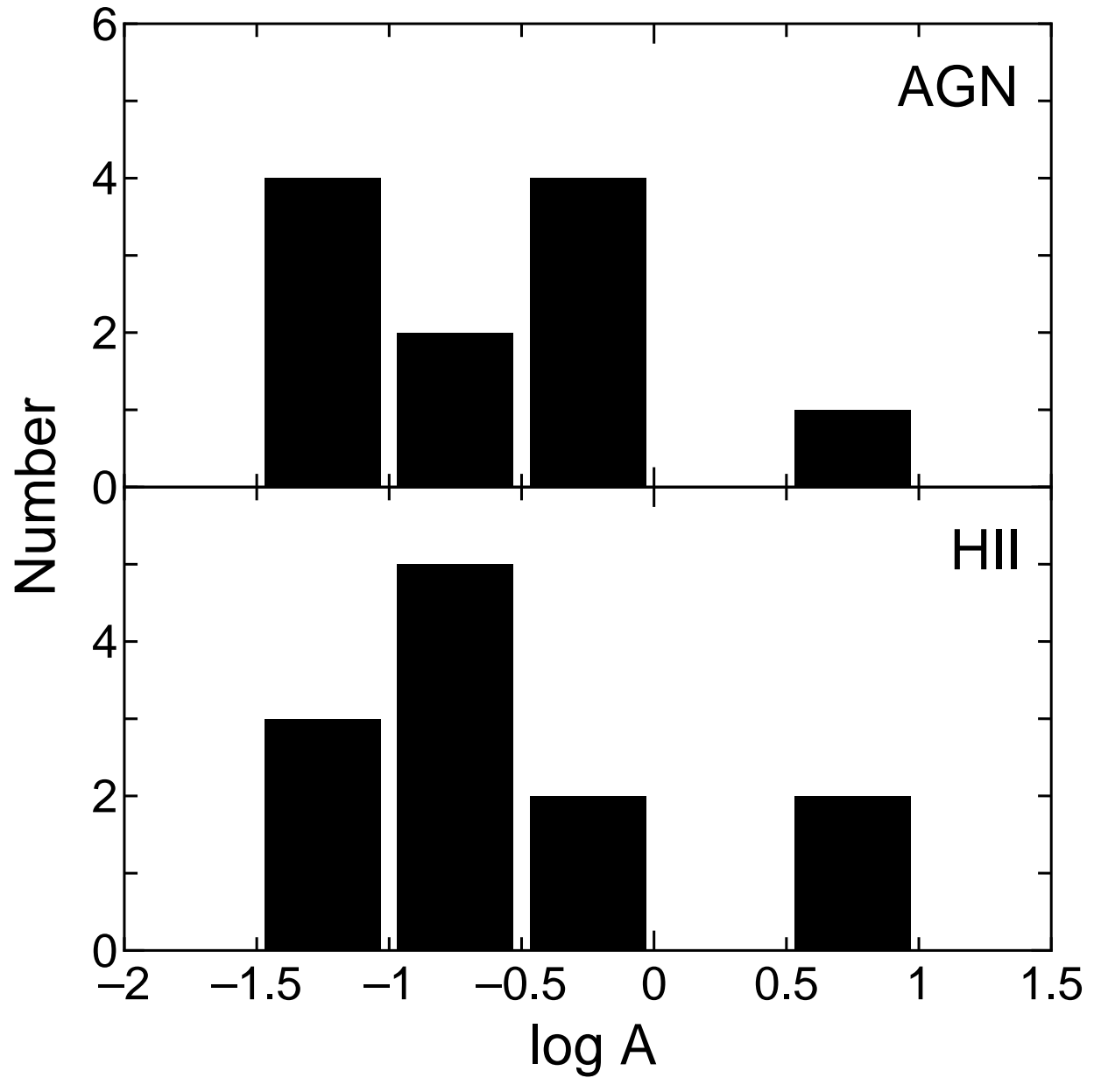


DISTANCE FROM NUCLEUS (R_{25})

ROTATION VELOCITY (km s^{-1})

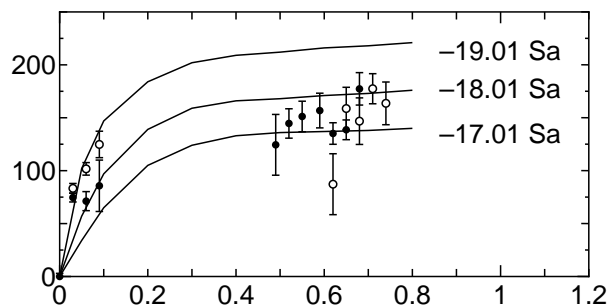


DISTANCE FROM NUCLEUS (arcsec)

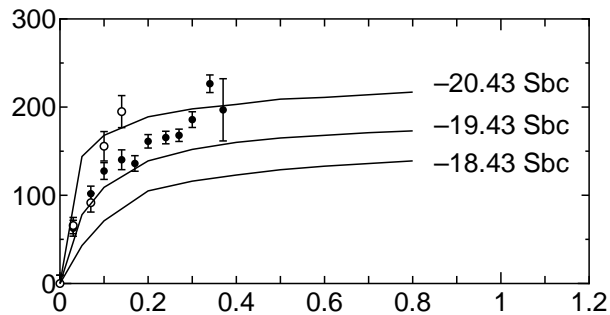


ROTATION VELOCITY (km s^{-1})

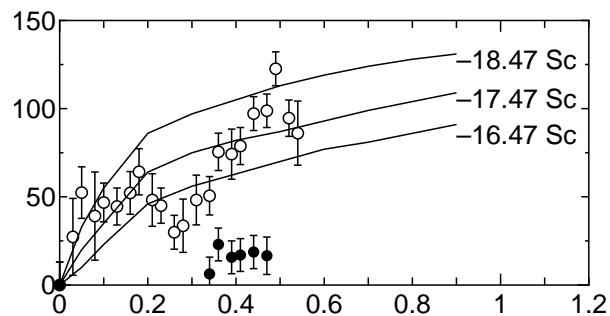
HCG 44c



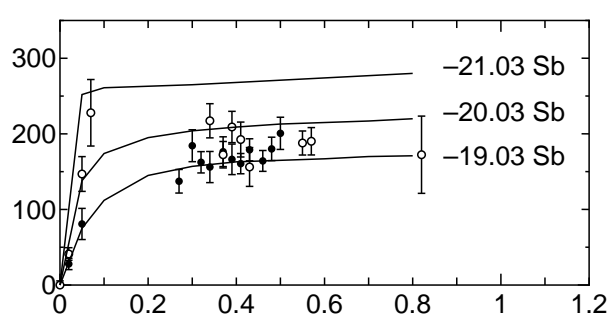
HCG 61c



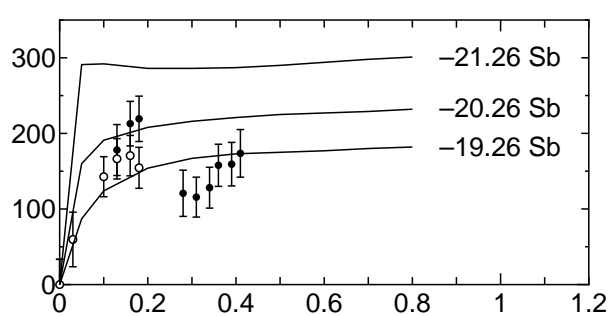
HCG 44d



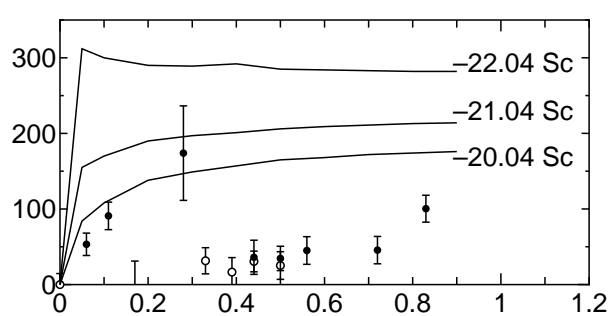
HCG 68c



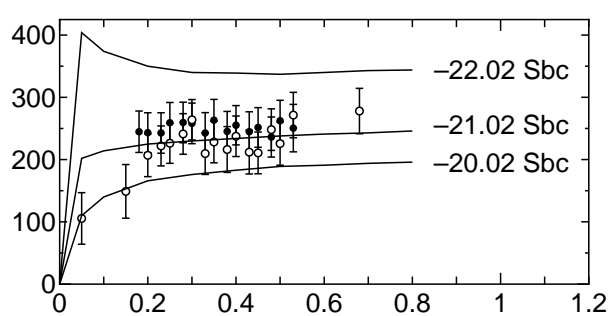
HCG 47a



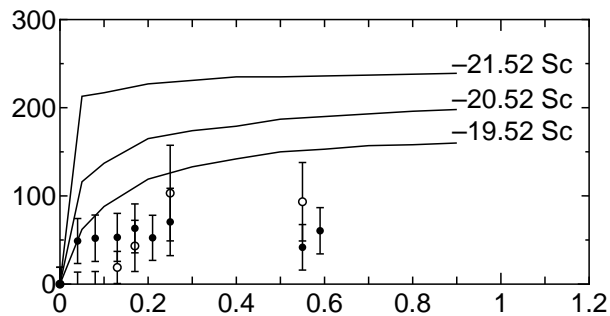
HCG 71a



HCG 53a

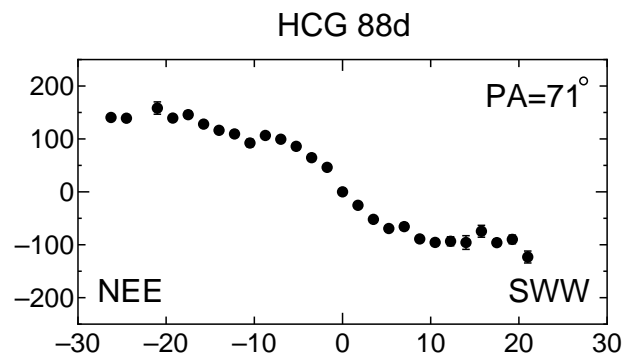
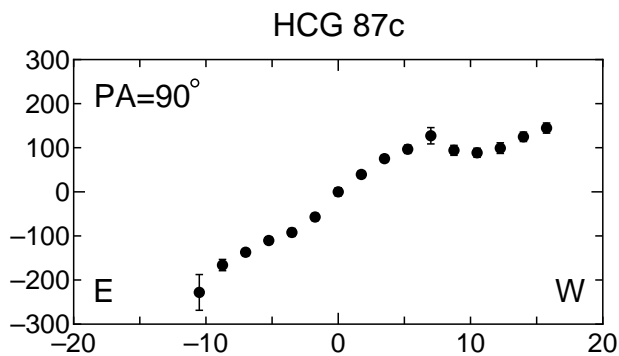
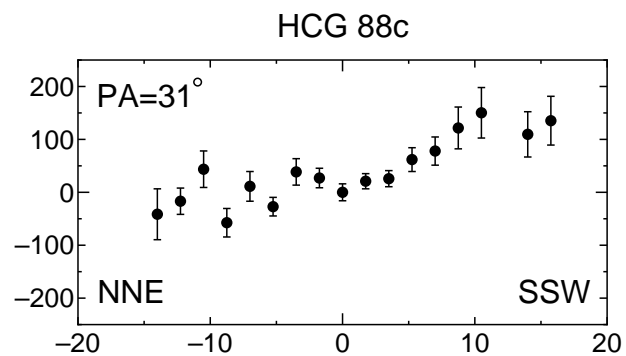
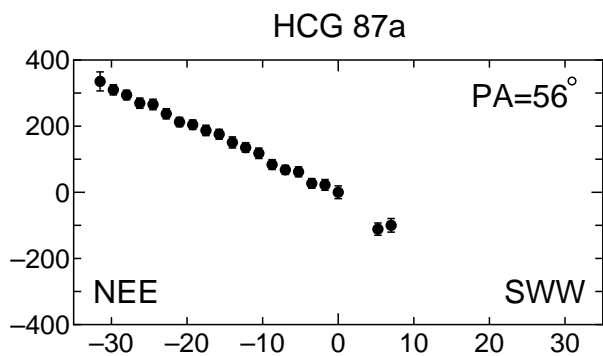
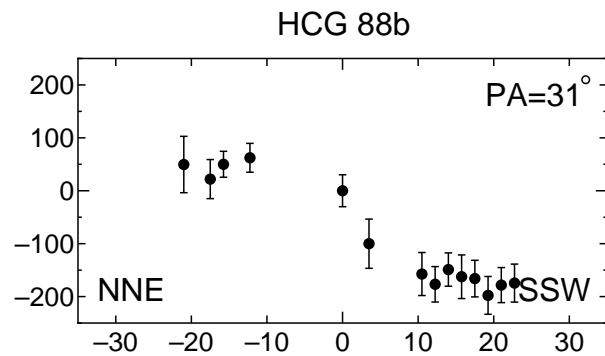
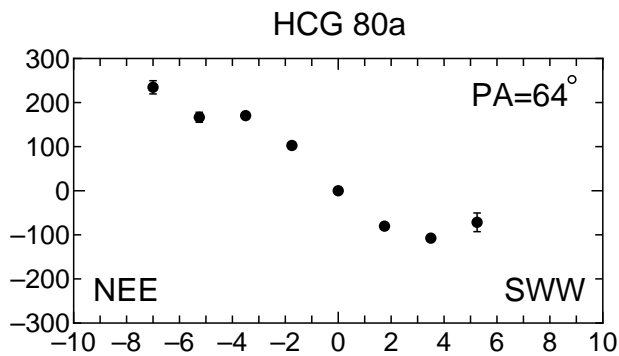
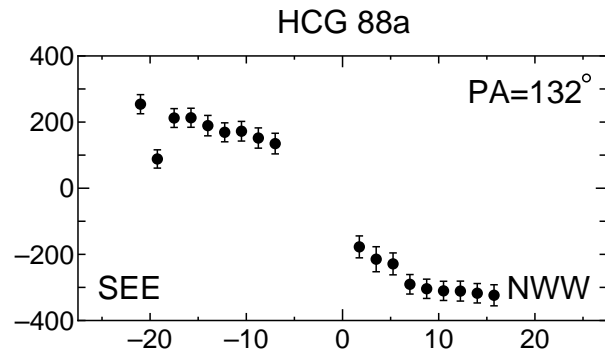
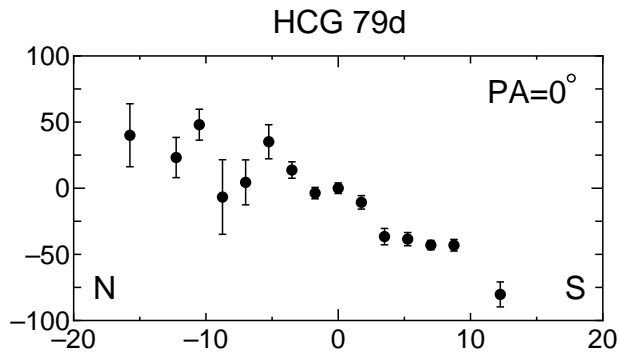


HCG 73a

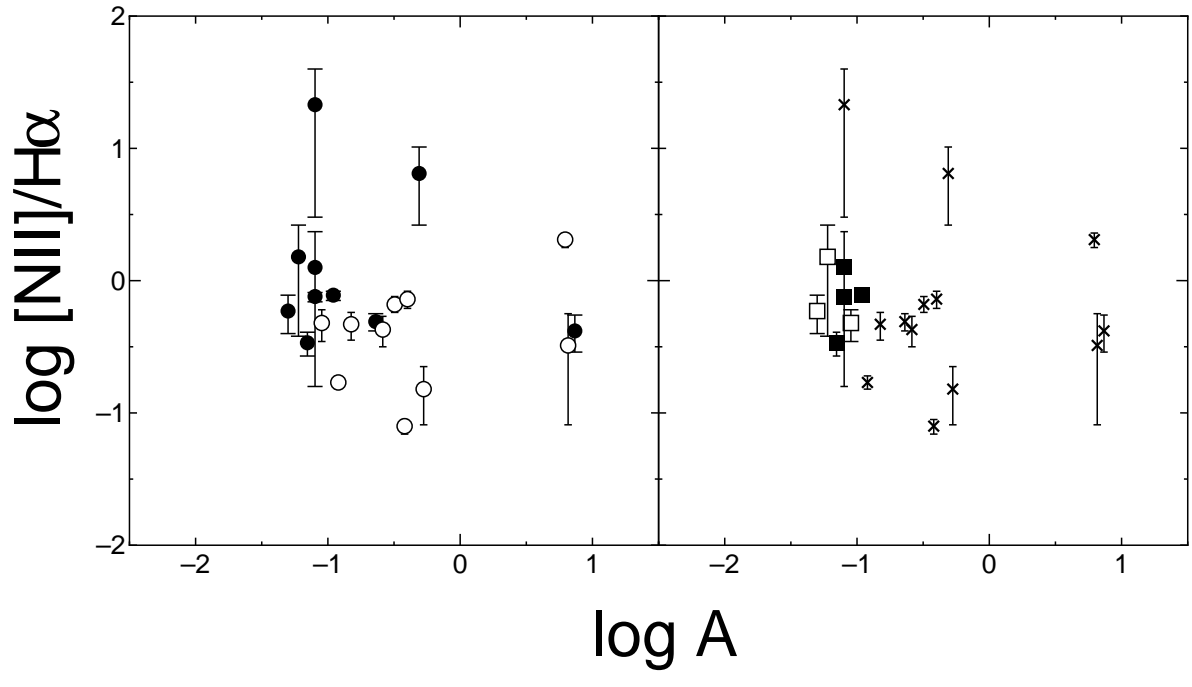


DISTANCE FROM NUCLEUS (R_{25})

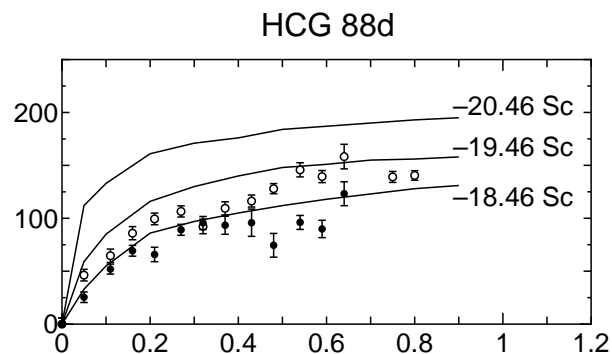
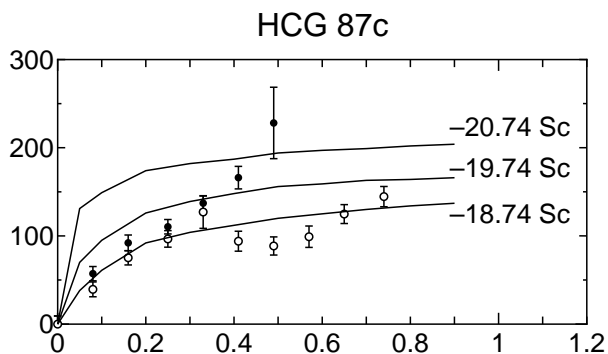
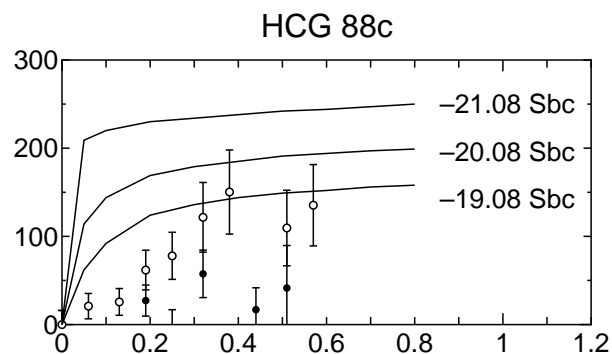
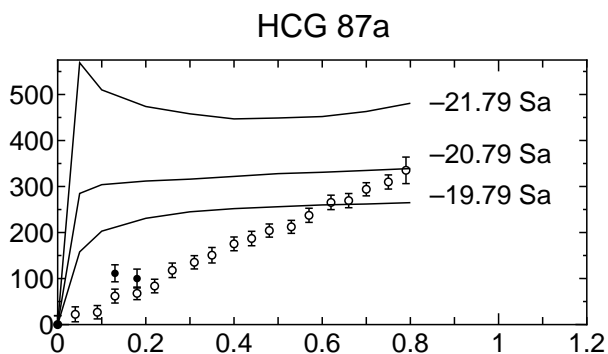
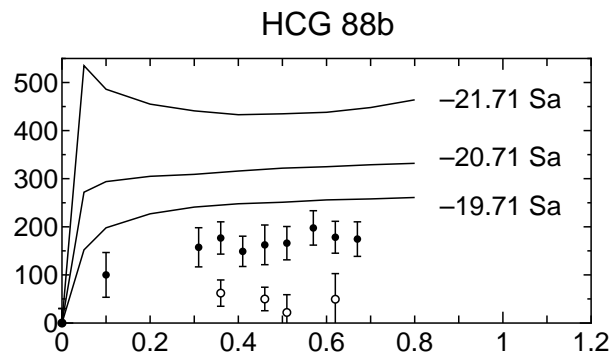
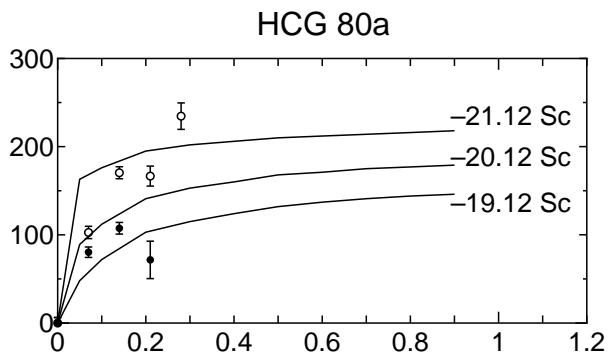
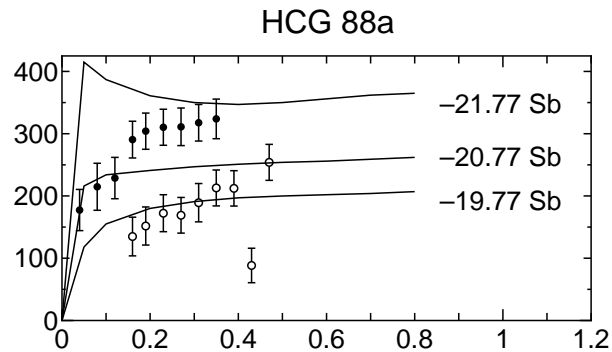
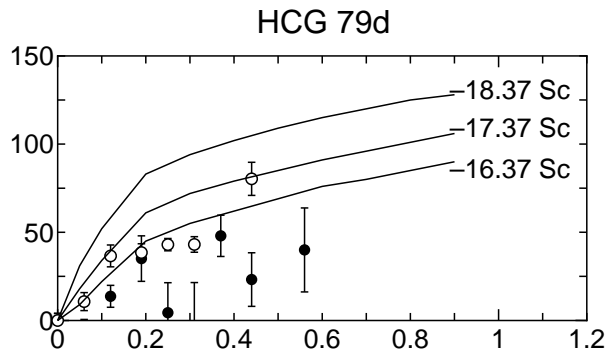
ROTATION VELOCITY (km s^{-1})



DISTANCE FROM NUCLEUS (arcsec)

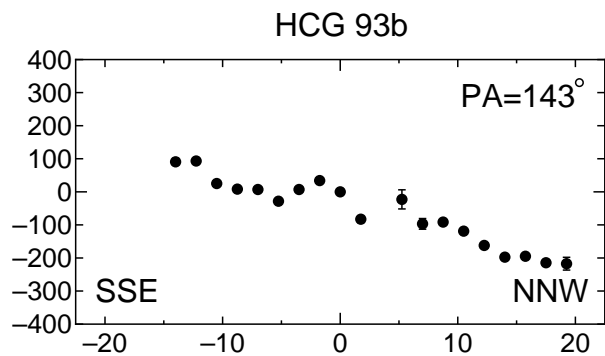
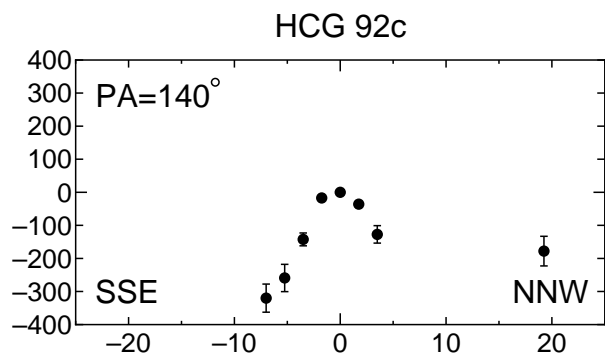
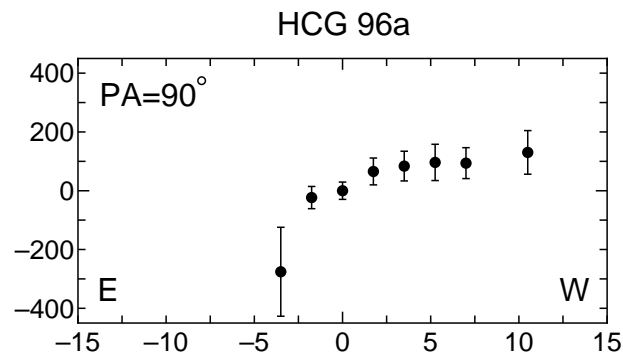
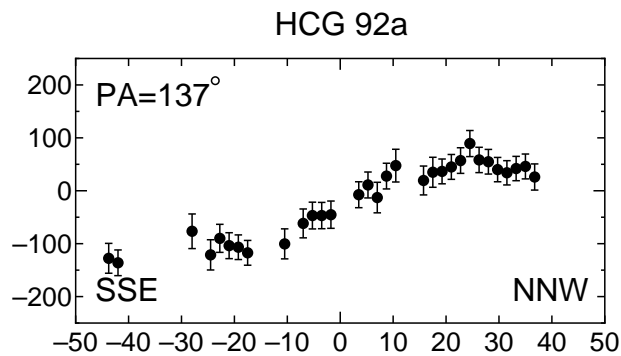
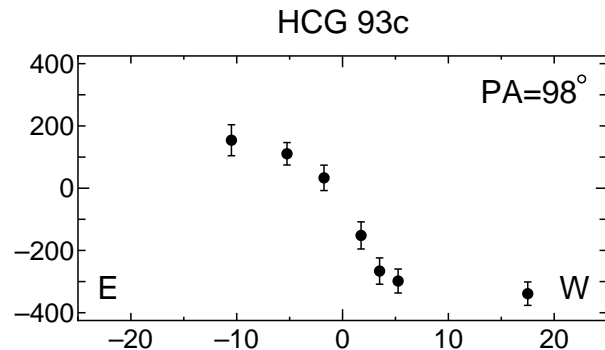
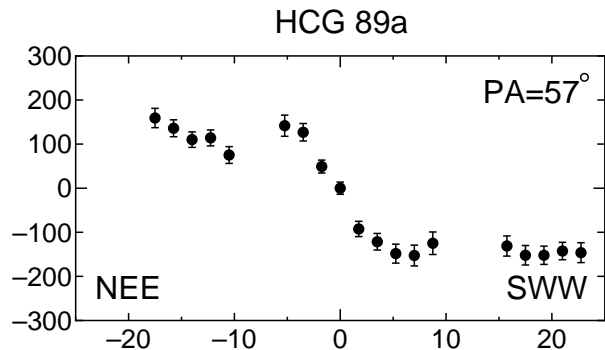


ROTATION VELOCITY (km s^{-1})

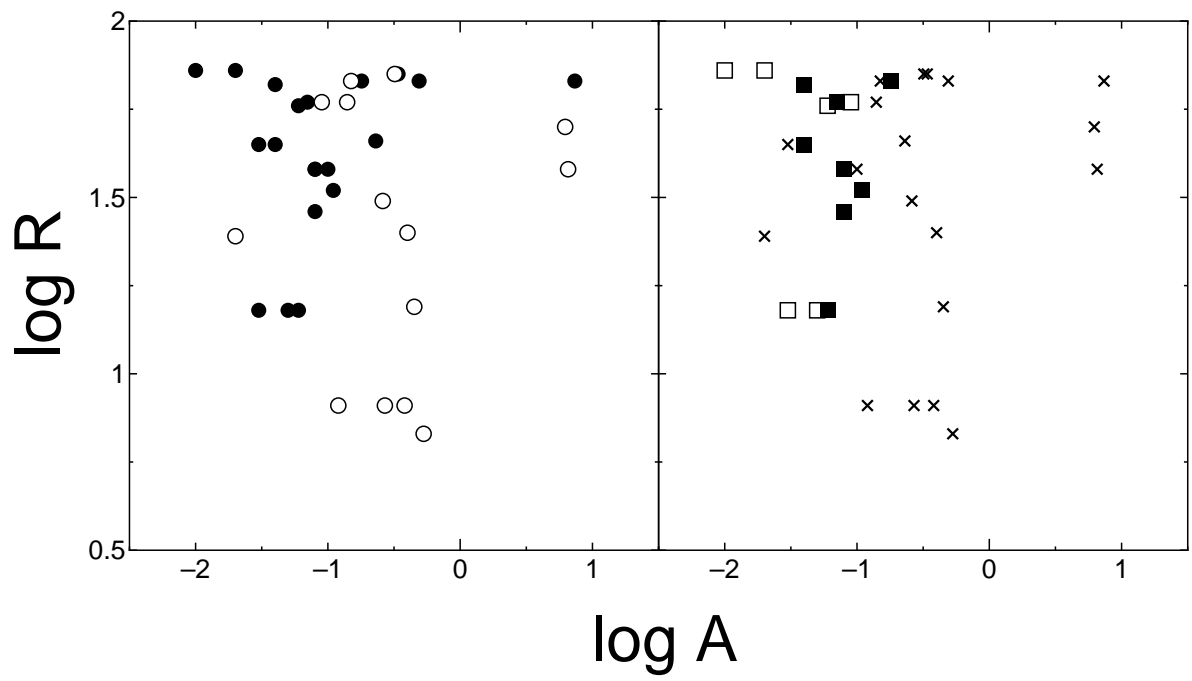


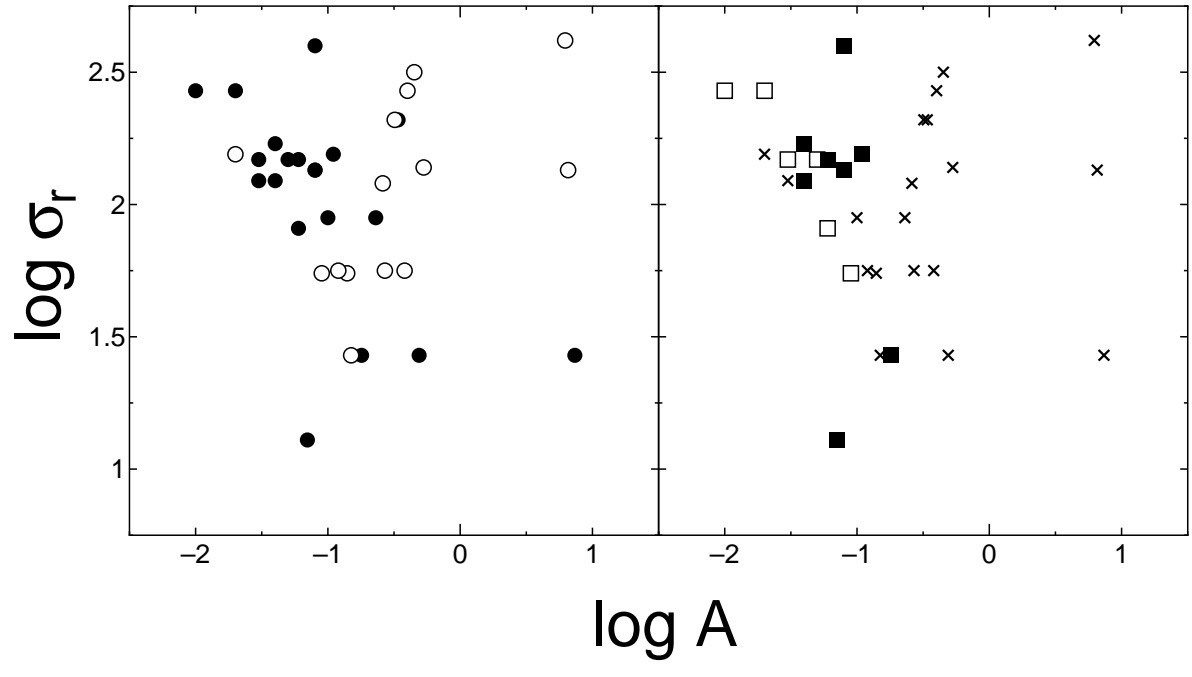
DISTANCE FROM NUCLEUS (R_{25})

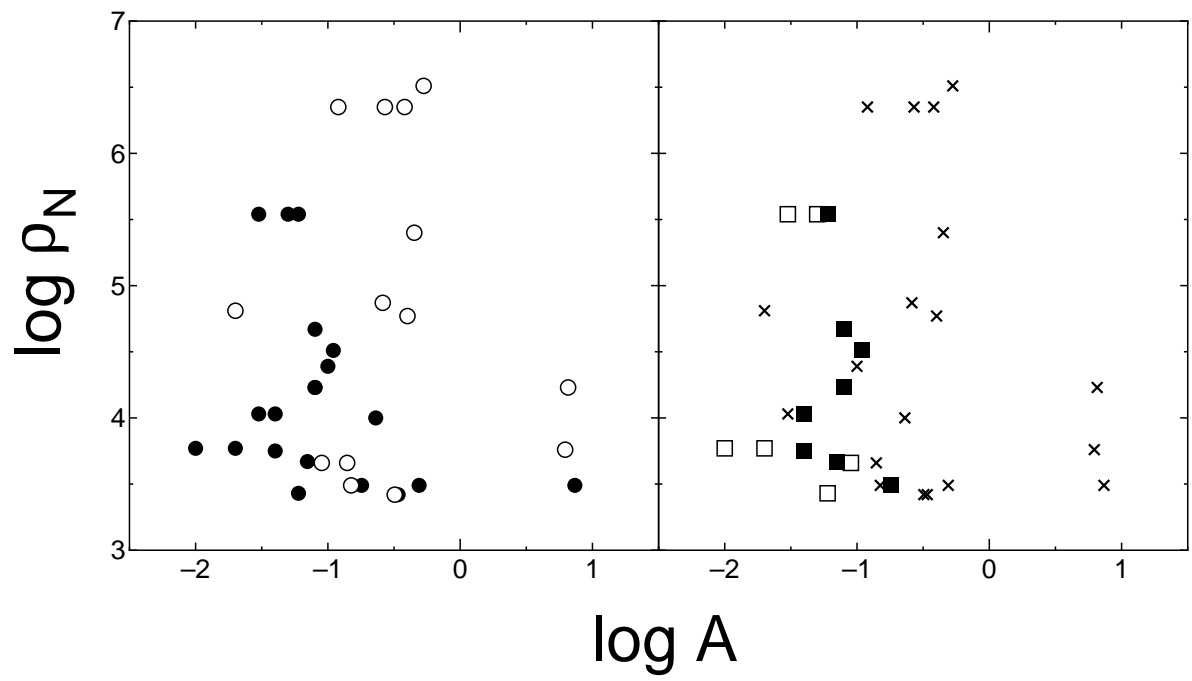
ROTATION VELOCITY (km s^{-1})

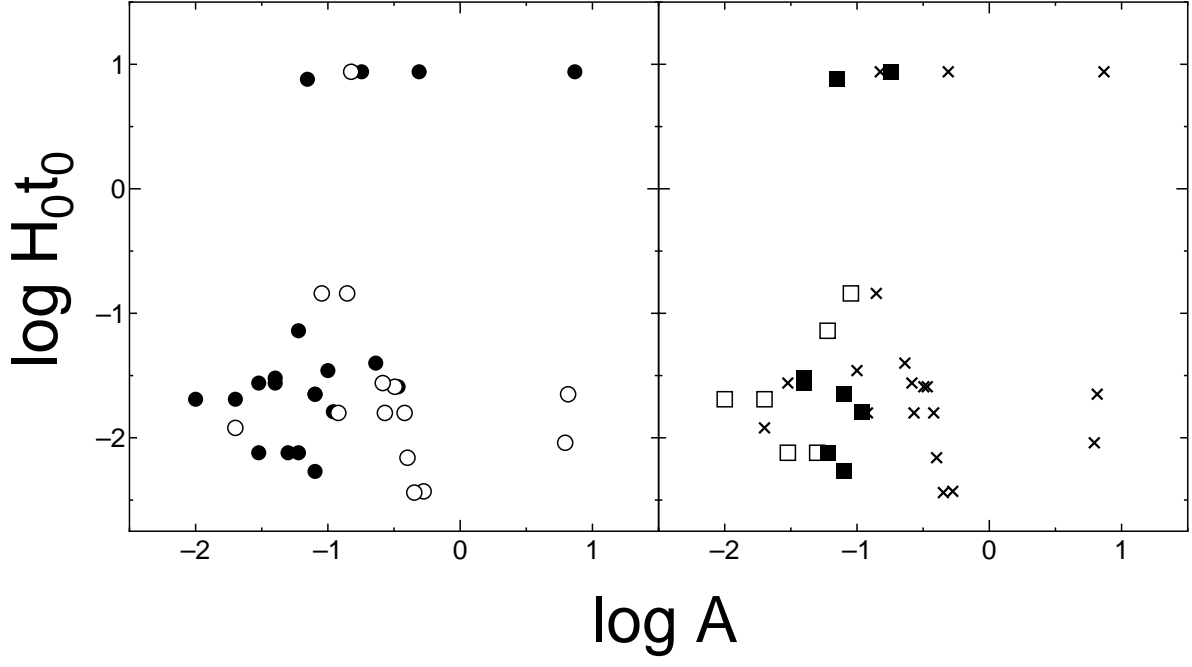


DISTANCE FROM NUCLEUS (arcsec)

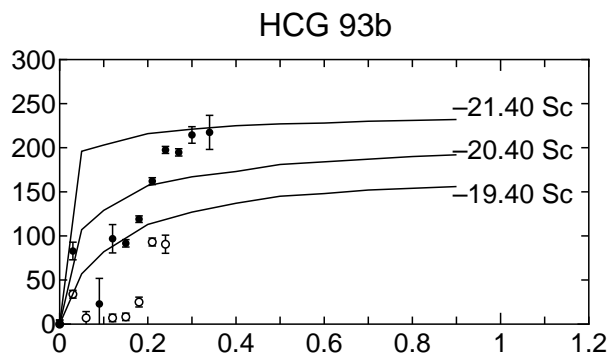
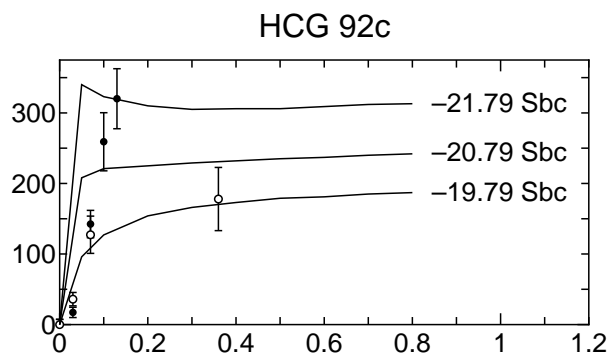
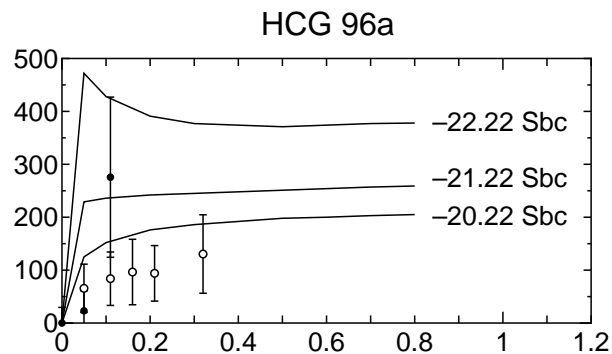
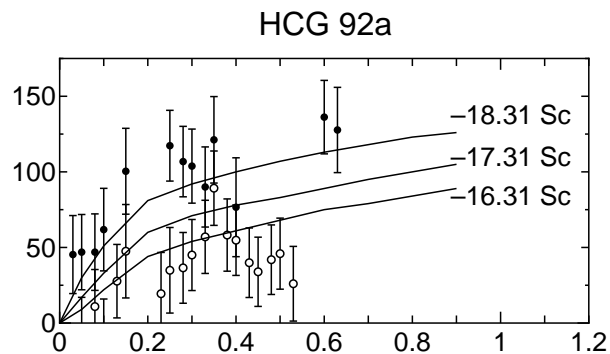
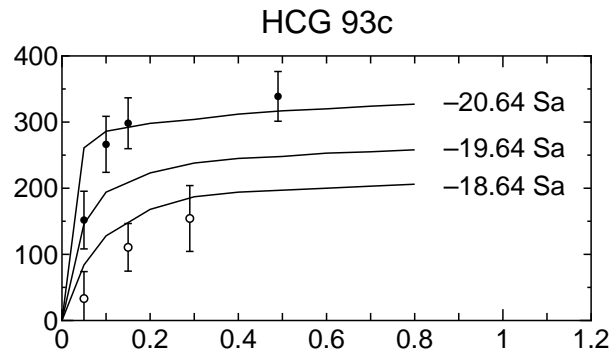
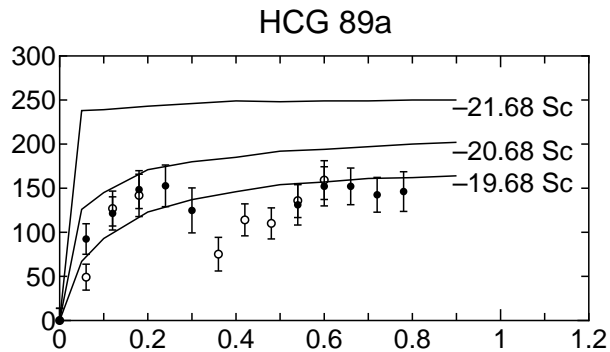




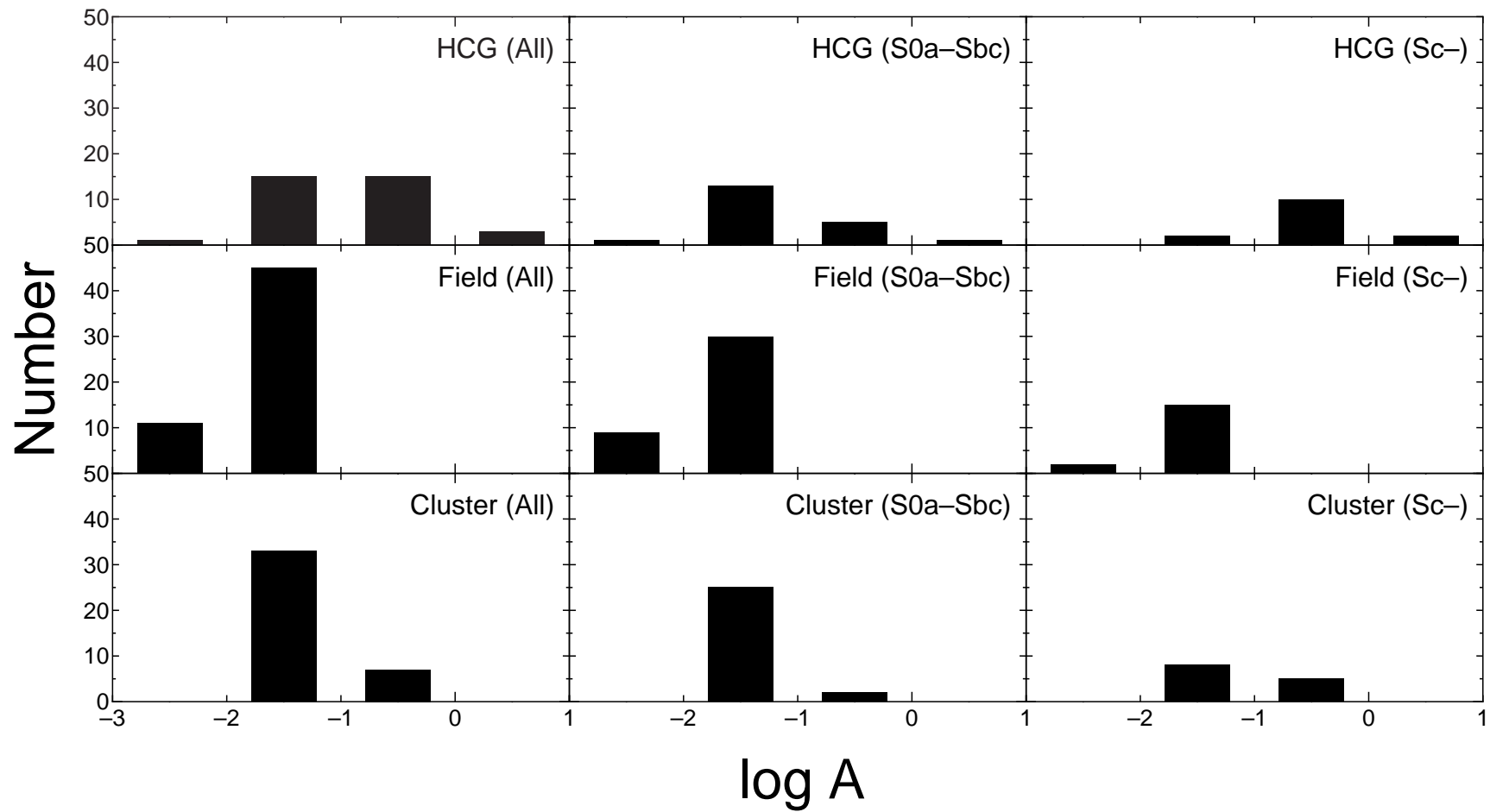




ROTATION VELOCITY (km s^{-1})



DISTANCE FROM NUCLEUS (R_{25})



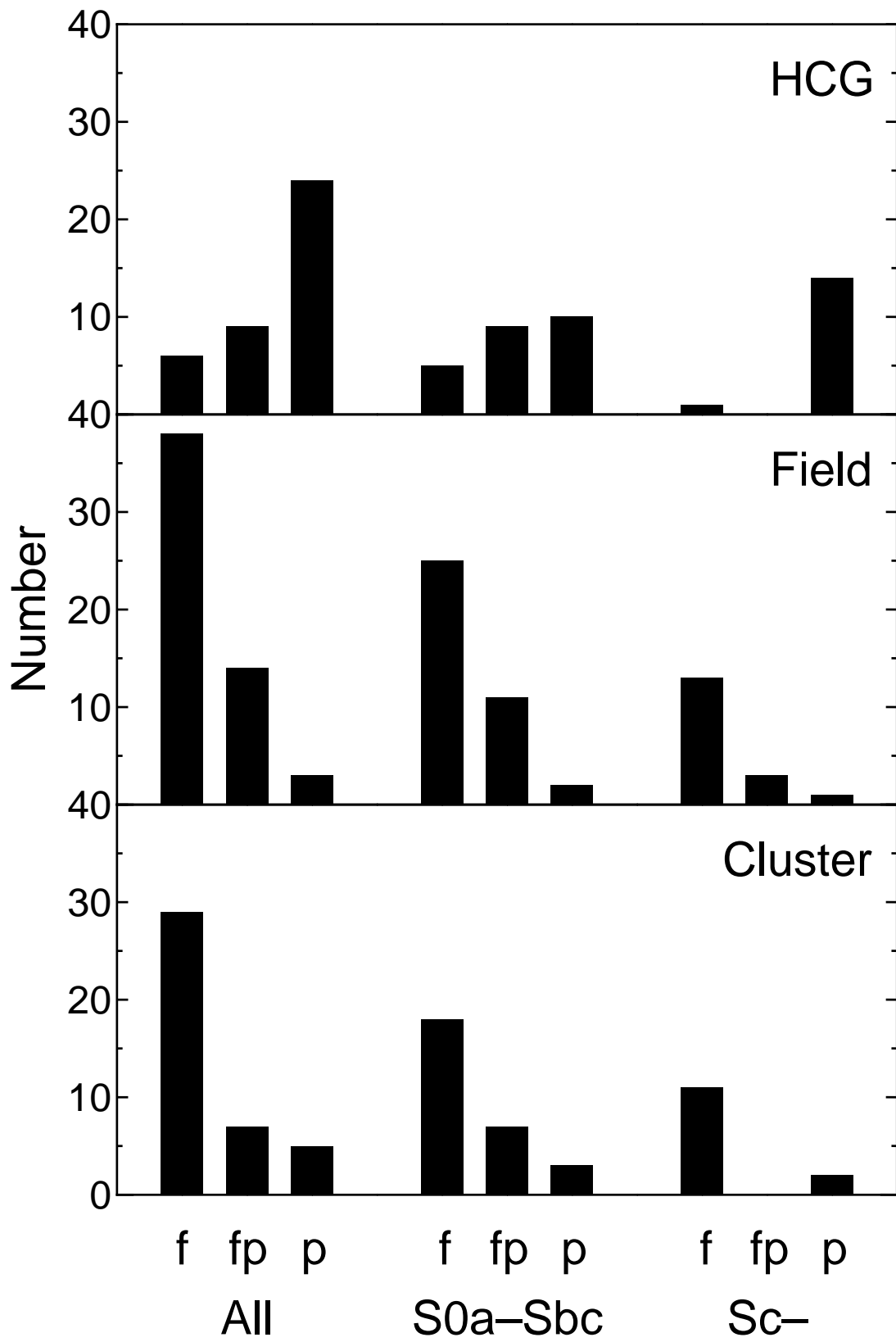


Table 1. A journal of observations

HCG	Date	Exp. (sec)	PA (deg)
7a	19 Aug 1996	1800	159
31a	09 Jan 1997	1800	80
31b	09 Jan 1997	1800	41
31c	09 Jan 1997	860	41
37b	21 Feb 1996	1800	77
38a	06 Jan 1997	1800	340
40c	23 Feb 1996	1800	122
44a	21 Feb 1996	1800	125
44c	21 Feb 1996	1800	130
44d	21 Feb 1996	1800	125
47a	21 Feb 1996	1800	15
53a	20 Feb 1996	1800	93
61c	21 Feb 1996	1800	130
68c	21 Feb 1996	1800	18
71a	20 Feb 1996	1800	23
73a ^a	25 Feb 1996	1800	18
79d	18 Aug 1996	1800	0
80a	25 Feb 1996	1800	64
87a ^b	18 Aug 1996	1800	56
87c	19 Aug 1996	1800	90
88a	15 Aug 1996	1800	132
88b	15 Aug 1996	1800	31

Table 1—Continued

HCG	Date	Exp. (sec)	PA (deg)
88c	15 Aug 1996	1800	31
88d	18 Aug 1996	1800	71
89a	19 Aug 1996	1800	57
92a ^a	15 Aug 1996	1800	137
92c	18 Aug 1996	1800	140
93b	19 Aug 1996	1800	143
93c	19 Aug 1996	1800	98
96a	19 Aug 1996	480	90

^aHCG 73a and 92a are redshift discordant galaxies, and we exclude these galaxies from statistical sample.

^bHCG 87a is classified into lenticular galaxy in RC3, and we exclude this galaxy from statistical sample.

Table 2. Properties of our HCG galaxies

HCG	Type (Hickson)	Type (RC3)	Type (Adopted)	V_{\odot} (km s ⁻¹)	$R_{\text{major}}^{\text{a}}$ (arcsec)	R_{minor} (arcsec)	$\sin i$
7a	Sb	(R')SB(r)a:	Sa	4133.3 ± 2.3	56.8	27.6	0.90 ± 0.02
31a	Sdm	Pec	P	4073.8 ± 0.9	32.3	19.9	0.88 ± 0.03
31b	Sm	S?	Sm	4136.3 ± 2.2	26.1	13.7	0.87 ± 0.00
31c	Im	S?	Im	4019.0 ± 0.3	18.3	7.0	0.94 ± 0.00
37b	Sbc	S?	Sbc	6786.9 ± 24.5	51.9	8.6	0.75 ± 0.10
38a	Sbc	S?	Sbc	8629.3 ± 8.1	22.1	8.6	0.99 ± 0.01
40c	Sbc	SB(rs)b pec	Sb	6406.2 ± 6.0	36.9	9.6	0.98 ± 0.01
44a	Sa	SA(s)a pec	Sa	(1293 \pm 24)	100.7	47.3	0.95 ± 0.01
44c	SBc	(R)SB(r)a	Sa	1217.1 ± 1.6	56.8	33.4	0.75 ± 0.03
44d	Sd	SB(s)c pec	Sc	1521.2 ± 8.5	67.7	27.4	0.92 ± 0.01
47a	SBb	SA(r):	Sb	9691.7 ± 19.6	26.3	17.9	0.80 ± 0.06
53a	SBbc	SB?	Sbc	(6261 \pm 31)	69.6	23.4	0.97 ± 0.01
61c	Sbc	S	Sbc	4012.4 ± 6.7	51.8	15.5	1.00 ± 0.01
68c	SBbc	SB(r)b	Sb	2299.6 ± 2.8	76.7	61.9	0.70 ± 0.05
71a	SBc	Scd:	Scd	9244.4 ± 9.1	31.5	25.8	0.85 ± 0.04
73a ^b	Scd	SA(s)c	Sc	5635.1 ± 6.9	41.5	30.8	0.50 ± 0.18
79d	Sdm	SB(s)c	Sc	4620.3 ± 2.9	28.1	12.3	1.00 ± 0.01
80a	Sd	S?	Sd	8975.1 ± 4.5	25.4	5.4	1.00 ± 0.00
87a ^c	Sbc	S0 ⁰ pec	S0	8443.4 ± 14.0	39.8	9.1	1.00 ± 0.00
87c	Sd	S?	Sd	8913.8 ± 6.5	21.4	9.1	0.97 ± 0.01
88a	Sb	Sb	Sb	(6033 \pm 25)	45.1	20.2	0.90 ± 0.03
88b	SBb	SB(r)a pec:	Sa	6192.1 ± 14.9	34.0	26.5	0.69 ± 0.10

Table 2—Continued

HCG	Type (Hickson)	Type (RC3)	Type (Adopted)	V_{\odot} (km s ⁻¹)	$R_{\text{major}}^{\text{a}}$ (arcsec)	R_{minor} (arcsec)	$\sin i$
88c	Sc	SAB(r)bc?	Sbc	5956.3 ± 6.2	27.6	21.0	0.54 ± 0.16
88d	Sc	S?	Sc	6041.5 ± 4.2	32.7	8.5	1.00 ± 0.01
89a	Sc	S?	Sc	8808.1 ± 7.8	29.1	16.1	0.78 ± 0.09
92a ^b	Sd	SA(s)d	Sd	(786 ± 20)	69.8	44.2	0.88 ± 0.02
92c	SBa	SB(s)bc pec	Sbc	6747.5 ± 3.6	52.8	41.5	0.67 ± 0.06
93b	SBd	SB(s)cd pec	Scd	4736.4 ± 3.2	57.4	19.5	0.98 ± 0.01
93c	SBa	(R)SAB(s)0/a pec	S0/a	(5132 ± 33)	35.9	15.9	0.92 ± 0.02
96a	Sc	SA(r)bc pec	Sbc	8671.3 ± 9.0	33.3	30.6	0.42 ± 0.19

^a R_{major} correspond to R_{25} .

^bHCG 73a and 92a are redshift discordant galaxies, and we exclude these galaxies from statistical sample.

^cHCG 87a is classified into lenticular galaxy in RC3, and we exclude this galaxy from statistical sample.

Table 3. The Asymmetry parameters and the shape parameter of the rotation curves for the observed galaxies

HCG	A	shape
7a	0.23	p
31a	0.12	p
31b	0.27	p
31c	0.38	p
37b		?
38a	0.07	fp
40c	0.09	f
44a	0.09	p
44c	0.13	fp
44d	6.55	p
47a		p
53a	0.06	f
61c		fp
68c	0.11	fp
71a	6.23	p
73a	0.18	p
79d	0.84	p
80a	0.40	p
87a		p
87c	0.26	p
88a	0.26	fp
88b	0.49	p
88c	1.21	p

Table 3—Continued

HCG	A	shape
88d	0.15	p
89a	0.14	fp
92a	0.41	p
92c		?
93b	0.32	p
93c	0.34	p
96a		p

Table 4. Properties of HCG galaxies from Rubin et al . (1991)

HCG	Type (Hickson)	Type (RC3)	Type (Adopted)	R_{25} (arcsec)	A	R. C. Type
16a	SBab	SAB(r)ab: pec	Sab	34.9	0.04	fp
16b	Sab	(R')Sa: pec	Sa	49.4	0.03	p
23b	SBc	(R)SAB(r)a pec	Sa	46.1	0.04	fp
31a ^a	Sdm	Pec	P	32.3		p
31b ^a	Sm	S?	Sm	26.1		p
31c ^a	Im	S?	Im	18.3		p
33c	Sd		Sd	23.3	0.02	p
34c	SBd		Sd	11.2	0.45	p
37b ^a	Sbc	S?	Sbc	51.9	0.08	fp
40c ^a	Sbc	SB(rs)b pec sp	Sb	36.9	0.01	f
40d	SBa	SB(s)0/a pec:	S0/a	23.9	0.06	fp
40e	Sc	SAB(s)a pec:	Sa	17.8	0.03	f
44a ^a	Sa	SA(s)a pec sp	Sa	100.7	0.07	p
44c ^a	SBc	(R)SB(r)a	Sa	56.8	0.03	fp
44d ^a	Sd	SB(s)c pec	Sc	67.7		p
57a	Sb	Sab sp pec	Sab	51.5		p
57b	SBb	SB(r)b	Sb	30.0	0.01	f
57d	SBc	SBb pec	Sb	17.3	0.02	f
79d ^a	Sdm	SB(s)c sp	Sc	28.1	0.21	p
88a ^a	Sb	Sb	Sb	45.1	0.10	fp
88c ^a	Sc	SAB(r)bc?	Sbc	27.6	13.5	p
89a ^a	Sc	S?	Sc	29.1	0.04	f

Table 4—Continued

HCG	Type (Hickson)	Type (RC3)	Type (Adopted)	R_{25} (arcsec)	A	R. C. Type
89b	SBc	S?	Sc	20.9	0.14	p
100a	Sb	S0/a	S0/a	33.2	0.10	p
100c	SBc	S?	Sc	22.1		p

^aHCG 31a, 31b, 31c, 37b, 40c, 44a, 44c, 44d, 79d, 88a, 88c, and 89a are commonly observed galaxies.

Table 5. Environments and nuclear activities of HCG galaxies

HCG	N	$\log R$	$\log \sigma_r$	$\log \rho_N$	$\log H_0 t_c$	Peculiar		Activity
		(kpc)	(km s ⁻¹)	(Mpc ⁻³)		Morphology	$\log[\text{NII}]/\text{H}\alpha$	
7a	4	1.66	1.95	4.00	-1.40	Y	$-0.31^{+0.06}_{-0.07}$	HII
16a	4	1.65	2.09	4.03	-1.56	Y		
16b	4	1.65	2.09	4.03	-1.56	Y		
23b	4	1.82	2.23	3.65	-1.52	Y		
31a	3	0.91	1.75	6.23	-1.80	Y	$-0.77^{+0.05}_{-0.05}$	HII
31b	3	0.91	1.75	6.23	-1.80	Y		HII
31c	3	0.91	1.75	6.23	-1.80	Y	$-1.10^{+0.05}_{-0.06}$	HII
33c	4	1.39	2.19	4.81	-1.92	N		
34c	4	1.19	2.50	5.40	-2.44	N		
37b	5	1.46	2.60	4.67	-2.27	Y	$0.10^{+0.27}_{-0.90}$	AGN
38a	3	1.77	1.11	3.55	0.88	Y	$-0.47^{+0.08}_{-0.10}$	HII
40c	5	1.18	2.17	5.54	-2.12	Y	$-0.23^{+0.12}_{-0.17}$	HII
40d	5	1.18	2.17	5.54	-2.12	Y		
40e	5	1.18	2.17	5.54	-2.12	Y		
44a	4	1.58	2.13	4.23	-1.65	Y	$1.33^{+0.27}_{-0.85}$	AGN
44c	4	1.58	2.13	4.23	-1.65	N	$-0.12^{+0.03}_{-0.04}$	AGN
44d	4	1.58	2.13	4.23	-1.65	Y	$-0.49^{+0.24}_{-0.60}$	HII
47a	4	1.56	1.63	4.30	0.66	Y		Abs
53a	3	1.76	1.91	3.31	-1.14	N	$0.18^{+0.24}_{-0.60}$	AGN
57a	7	1.86	2.43	3.71	-1.69	Y	$0.14^{+0.19}_{-0.33}$	AGN
57b	7	1.86	2.43	3.71	-1.69	Y		
57d	7	1.86	2.43	3.71	-1.69	Y		

Table 5—Continued

HCG	N	$\log R$ (kpc)	$\log \sigma_r$ (km s ⁻¹)	$\log \rho_N$ (Mpc ⁻³)	$\log H_0 t_c$	Peculiar Morphology	$\log[\text{NII}]/\text{H}\alpha$	Activity
61c	3	1.46	1.94	4.49	-1.60	Y	$-0.14^{+0.06}_{-0.07}$	AGN
68c	5	1.52	2.19	4.51	-1.79	Y	$-0.11^{+0.03}_{-0.04}$	AGN
71a	3	1.70	2.62	3.64	-2.04	N	$0.31^{+0.05}_{-0.06}$	AGN
79d	4	0.83	2.14	6.51	-2.43	Y	$-0.82^{+0.17}_{-0.27}$	HII
80a	4	1.40	2.43	4.77	-2.16	N	$-0.14^{+0.06}_{-0.07}$	AGN
87c	3	1.49	2.08	4.75	-1.56	Y	$-0.37^{+0.10}_{-0.13}$	HII
88a	4	1.83	1.43	3.49	0.94	N		AGN
88b	4	1.83	1.43	3.49	0.94	Y	$0.81^{+0.20}_{-0.39}$	AGN
88c	4	1.83	1.43	3.49	0.94	N	$-0.38^{+0.12}_{-0.16}$	HII
88d	4	1.83	1.43	3.49	0.94	N	$-0.33^{+0.09}_{-0.12}$	HII
89a	4	1.77	1.74	3.66	-0.84	N	$-0.32^{+0.10}_{-0.14}$	HII
89b	4	1.77	1.74	3.66	-0.84	N		
92c	4	1.45	2.59	4.62	-2.27	Y	$0.16^{+0.03}_{-0.03}$	AGN
93b	4	1.85	2.32	3.42	-1.59	Y	$-0.18^{+0.06}_{-0.06}$	AGN
93c	4	1.85	2.32	3.42	-1.59	Y		AGN
96a	4	1.48	2.12	4.54	-1.76	Y	$-0.00^{+0.08}_{-0.10}$	AGN
100a	3	1.58	1.95	4.27	-1.46	Y		
100c	3	1.58	1.95	4.27	-1.46	N		

Table 6. Comparison of kinematical properties with morphological peculiarities

Morphology	Rotation Curves		
	f	fp	p
normal	2	2	8
peculiar	4	7	16
$P(\chi^2)^a$		0.818	

^aThe possibility that rejects the null hypothesis.

Table 7. A summary of the Spearman rank test for the correlations between asymmetry parameter A and the $[\text{NII}]/\text{H}\alpha$ ratio

	Number	Probabilities ^a
All	20	0.243
S0/a–Sbc	10	0.987
Sc _≤	10	0.907
f	3	0.667
fp	4	0.200
p	13	0.566

^aThe probability that rejects the null hypothesis.

Table 8. A summary of the Spearman rank test for the correlations between asymmetry parameter A and the properties of the HCGs

	Number	$\log R$	Probabilities ^a		
			$\log \sigma_r$	$\log \rho_N$	$\log H_0 t_c$
All	34	0.737	0.355	0.748	0.804
S0/a–Sbc	20	0.686	0.052	0.135	0.028
Sc \leq	14	0.543	0.037	0.533	0.085
f	6	0.329	4.81×10^{-3}	0.397	0.266
fp	8	0.955	1.000	0.867	1.000
p	20	0.701	0.519	0.762	0.565

^aThe probability that rejects the null hypothesis.

Table 9. Properties of Field Spiral Galaxies

Name	Type RC3	Type Adopted	R_{25} (arcsec)	A	R. C. Type	Ref. ^a
NGC0701	SB(rs)c	Sc	73.6	0.02	p	1
NGC0753	SAB(rs)bc	Sbc	75.4	0.02	f	1
NGC0801	Sc	Sc	94.9	0.01	f	1
NGC1024	(R')SA(r)ab	Sab	117	0.01	fp	3
NGC1035	SA(s)c	Sc	67.2	0.02	f	1
NGC1085	SA(s)bc:	Sbc	88.5	0.01	f	2
NGC1087	SAB(rs)c	Sc	112	0.02	f	1
NGC1325	SA(s)bc	Sbc	140	0.01	f	2
NGC1357	SA(s)ab	Sab	84.6	0.03	fp	3
NGC1417	SAB(rs)b	Sb	80.8	0.01	f	2
NGC1421	SAB(rs)bc:	Sbc	106	0.04	f	1
NGC1515	SAB(rs)bc	Sbc	157	0.02	f	2
NGC1620	SA(s)bc	Sbc	86.5	0.01	f	2
NGC2590	SA(s)bc:	Sbc	67.2	0.01	f	2
NGC2608	SB(s)b:	Sb	68.7	0.00	fp	1
NGC2639	(R)SA(r)a	Sa	54.6	0.01	f	3
NGC2708	SAB(s)b pec:	Sb	78.9	0.01	fp	2
NGC2715	SAB(rs)c	Sc	147	0.01	f	1
NGC2742	SA(s)c	Sc	90.6	0.02	f	1
NGC2775	SA(r)ab	Sab	128	0.01	f	3
NGC2815	SB(r)b:	Sb	104	0.01	f	2
NGC2844	SA(r)a:	Sa	46.5	0.02	f	3

Table 9—Continued

Name	Type RC3	Type Adopted	R_{25} (arcsec)	A	R. C. Type	Ref. ^a
NGC2998	SAB(rs)c	Sc	86.5	0.01	f	1
NGC3054	SAB(r)b	Sb	114	0.06	fp	2
NGC3067	SAB(s)ab	Sab	73.6	0.01	f	2
NGC3145	SB(rs)bc	Sbc	92.7	0.02	f	2
NGC3200	SAB(rs)c:	Sc	125	0.01	fp	2
NGC3223	SA(s)b	Sb	122	0.01	fp	2
NGC3281	SA(s)ab pec:	Sab	99.3	0.03	fp	3
NGC3495	Sd:	Sd	147	0.02	f	1
NGC3593	SA(s)0/a:	S0/a	157	0.03	?	3
NGC3672	SA(s)c	Sc	125	0.04	f	1
NGC3898	SA(s)ab	Sab	131	0.01	f	3
NGC4062	SA(s)c	Sc	122	0.01	f	1
NGC4378	(R)SA(s)a	Sa	84.6	0.02	fp	3
NGC4594	SA(s)a sp	Sa	261	0.01	fp	3
NGC4605	SB(s)c pec	Sc	173	0.03	f	1
NGC4682	SAB(s)cd	Scd	77.1	0.04	f	1
NGC4698	SA(s)ab	Sab	119	0.02	p	3
NGC4800	SA(rs)b	Sb	47.5	0.01	f	2
NGC4845	SA(s)ab sp	Sab	150	0.04	f	3
NGC6314	SA(s)a: sp	Sa	43.4	0.01	f	3
NGC7083	SA(s)bc	Sbc	117	0.03	f	2
NGC7171	SB(rs)b	Sb	78.9	0.06	f	2

Table 9—Continued

Name	Type RC3	Type Adopted	R_{25} (arcsec)	A	R. C. Type	Ref. ^a
NGC7217	(R)SA(r)ab	Sab	117	0.01	f	2
NGC7537	SAbc:	Sbc	67.2	0.02	f	2
NGC7541	SB(rs)bc pec	Sbc	104	0.02	fp	1
NGC7606	SA(s)b	Sb	161	0.01	f	2
NGC7664	Sc:	Sc	78.9	0.01	f	1
IC467	SAB(s)c	Sc	97.1	0.03	fp	1
IC724	Sa	Sa	70.3	0.00	f	3
UGC02885	SA(rs)c	Sc	117	0.01	fp	1
UGC03691	SACd	Scd	65.6	0.03	f	1
UGC10205	Sa	Sa	43.4	0.02	p	3
UGC11810	SAB(r)bc:	Sbc	54.6	0.02	fp	2
UGC12810	(R')SAB(r)bc pec	Sbc	55.9	0.02	f	2

^a1: Rubin et al. (1980), 2: Rubin et al. (1982), and 3: Rubin et al. (1985)

Table 10. Results of KS test for distributions of the asymmetry parameter between the HCG spiral galaxies and the field spiral galaxies

	KS Probability ^a
All HCG vs. All Field	1.15×10^{-11}
HCG S0/a-Sbc vs. Field S0/a-Sbc	1.76×10^{-6}
HCG Sc- vs. Field Sc-	7.40×10^{-7}
HCG S0/a-Sbc vs. HCG Sc-	2.32×10^{-3}
Field S0/a-Sbc vs. Field Sc-	0.792

^aThe possibility that rejects the null hypothesis.

Table 11. Frequency distributions of the rotation curve shape between the HCGs spiral galaxies and the field spiral galaxies^a

	All ^b		S0a-Sbc		Sc-	
	HCGs	Field	HCGs	Field	HCGs	Field
f	15.4 (6)	69.1 (38)	20.8 (5)	65.8 (25)	6.7 (1)	76.5 (13)
fp	23.1 (9)	25.5 (14)	37.5 (9)	28.9 (11)	0.0 (0)	17.6 (3)
p	61.5 (24)	5.5 (3)	41.7 (10)	5.3 (2)	93.3 (14)	5.9 (1)
$P(\chi^2)^c$	3.23×10^{-9}		2.55×10^{-4}		4.73×10^{-6}	

^aNumbers in parentheses are the actual numbers.

^b“All” means that the total sample of S0a–Sbc, and Sc- galaxies .

^cThe possibility that rejects the null hypothesis.

Table 12. Properties of cluster Spiral Galaxies

Galaxy Name	Cluster Name	Type RC3	Type Adopted	R_{25} (arcsec)	A	R.C.Type	Ref. ^a
NGC0668	A262	Sb	Sb	55.9	0.04	f	1
NGC0669	A262	Sab	Sab	97.1	0.11	p	1
NGC0688	A262	(R')SAB(rs)b	Sb	75.4	0.03	fp	1
UGC01347	A262	SAB(rs)c	Sc	39.5	0.07	f	1
NGC0753	A262	SAB(rs)bc	Sbc	78.9	0.04	fp	1
UGC01493	A262	SBab?	Sab	57.2	0.04	f	1
UGC03269	A539	Sbc	Sbc	27.4	0.02	f	2
UGC03282	A539	SBcd?	Scd	33.7	0.11	f	2
Z119-051	Cancer		Sb	16.4	0.03	f	1, 3
Z119-043	Cancer		Im	18.1	0.04	p	2, 3
UGC04329	Cancer	SA(r)cd	Scd	62.7	0.11	p	2
NGC2558	Cancer	SAB(rs)ab	Sab	54.6	0.01	f	2
Z119-053	Cancer		S0a	20.9	0.04	f	2, 3
UGC04386	Cancer	Sb	Sb	57.2	0.07	p	2
NGC2595	Cancer	SAB(rs)c	Sc	97.1	0.05	f	2
NGC3861	A1367	(R')SAB(r)b	Sb	68.7	0.06	fp	1
NGC3883	A1367	SA(rs)b	Sb	88.5	0.05	f	1
UGC08161	Coma	S?	Sb	32.2		?	1, 3
NGC4848	Coma	SBab: sp	Sab	48.7	0.07	f	2
Z160-058	Coma	S?	Sbc	31.4	0.02	f	2, 3
NGC4911	Coma	SAB(r)bc	Sbc	43.4	0.05	f	2

Table 12—Continued

Galaxy Name	Cluster Name	Type RC3	Type Adopted	R_{25} (arcsec)	A	R.C.Type	Ref. ^a
NGC4921	Coma	SB(rs)ab	Sab	73.6	0.10	p	2
Z130-008	Coma	S?	Sc	12.8	0.03	f	2, 3
IC1179	Hercules	SB(rs)cd	Scd	17.7	0.13	f	1
NGC6050	Hercules	SA(s)c	Sc	26.1	0.01	f	1
NGC6054	Hercules	(R')SAB(s)b	Sb	20.8	0.04	f	1
UGC10085	Hercules	SAcd:	Scd	31.4	0.08	f	2
NGC6045	Hercules	SB(s)c sp	Sc	40.5	0.12	f	2
NGC7591	Pegasus	SBbc	Sbc	59.9	0.02	f	1
NGC7536	Pegasus	SBbc	Sbc	59.9	0.05	f	2
NGC7593	Pegasus	S?	Sc	31.4	0.02	f	2
UGC12498	Pegasus	Sb	Sb	42.4	0.05	f	2
NGC7631	Pegasus	SA(r)b:	Sb	55.9	0.02	f	2
NGC7643	Pegasus	S?	Sc	43.4	0.02	f	2
IC4755	DC1842-63		Sb	39.4	0.05	fp	4, 5
IC4764	DC1842-63	S?	Sa	39.6	0.06	fp	4, 5
IC4770	DC1842-63	(R)SAB(rs)a:	Sa	26.1	0.10	fp	4
IC4771	DC1842-63	SA(rs)bc:	Sbc	36.9	0.06	f	4
IC4769	DC1842-63	(R')SB(s)b pec	Sb	61.3	0.08	fp	4
IC4759	DC1842-63		Im	22.5	0.14	f	4, 5
IC4741	DC1842-63	SA(r)ab	Sab	46.5	0.02	f	4

^a1: Amram et al. (1994), 2: Amram et al. (1992), 3: Gavazzi & Boselli (1996), 4: Amram et al. (1995), 5: Bell & Whitmore (1989)

Table 13. Results of KS test for distributions of the asymmetry parameter between the HCG spiral galaxies and the cluster spiral galaxies

	KS Probability ^a
All HCG vs. All Cluster	6.64×10^{-4}
HCG S0/a-Sbc vs. Cluster S0/a-Sbc	4.50×10^{-2}
HCG Sc- vs. Cluster Sc-	8.48×10^{-4}
HCG S0/a-Sbc vs. HCG Sc-	2.32×10^{-3}
Cluster S0/a-Sbc vs. Cluster Sc-	0.183

^aThe possibility that rejects the null hypothesis.

Table 14. Frequency distributions of the rotation curve shape between the HCGs spiral galaxies and the clusters spiral galaxies^a

	All ^b		S0a-Sbc		Sc-	
	HCGs	Clusters	HCGs	Clusters	HCGs	Clusters
f	15.4 (6)	70.7 (29)	20.8 (5)	64.3 (18)	6.7 (1)	84.6 (11)
fp	23.1 (9)	17.1 (7)	37.5 (9)	25.0 (7)	0.0 (0)	0.0 (0)
p	61.5 (24)	12.2 (5)	41.7 (10)	10.7 (3)	93.3 (14)	15.4 (2)
$P(\chi^2)^c$	9.28×10^{-7}		3.84×10^{-3}		3.23×10^{-5}	

^aNumbers in parentheses are the actual numbers.

^b“All” means that the total sample of S0a–Sbc, and Sc- galaxies .

^cThe possibility that rejects the null hypothesis.

Table 15. Velocities for spirals in Hickson compact groups

r (arcsec)	r/R_{25}	$V(r)$ (km s ⁻¹)	$dV(r)$ (km s ⁻¹)
HCG 7a			
-28.00	-0.49	-128	13
-26.25	-0.46	-144	14
-24.50	-0.43	-150	8
-22.75	-0.40	-135	7
-21.00	-0.37	-133	6
-19.25	-0.34	-127	6
-17.50	-0.31	-133	9
-5.25	-0.09	-145	12
-3.50	-0.06	-133	5
-1.75	-0.03	-86	4
0.00	0.00	0	4
1.75	0.03	116	5
3.50	0.06	209	7
5.25	0.09	238	9
7.00	0.12	193	14
15.75	0.28	192	11
19.25	0.34	205	8
21.00	0.37	228	9
22.75	0.40	226	7
24.50	0.43	210	10

Table 15—Continued

r (arcsec)	r/R_{25}	$V(r)$ (km s ⁻¹)	$dV(r)$ (km s ⁻¹)
26.25	0.46	243	10
28.00	0.49	230	9
29.75	0.52	222	10
HCG 31a			
-14.00	-0.43	85	15
-12.25	-0.38	69	11
-10.50	-0.33	52	5
-8.75	-0.27	60	3
-7.00	-0.22	58	3
-5.25	-0.16	52	3
-3.50	-0.11	37	3
-1.75	-0.05	9	2
0.00	0.00	0	1
3.50	0.11	-30	2
5.25	0.16	-49	3
7.00	0.22	-54	3
8.75	0.27	-65	3
10.50	0.33	-81	4
12.25	0.38	-93	4
14.00	0.43	-88	4
15.75	0.49	-84	7

Table 15—Continued

r (arcsec)	r/R_{25}	$V(r)$ (km s ⁻¹)	$dV(r)$ (km s ⁻¹)
17.50	0.54	-50	6
HCG 31b			
-21.00	-0.80	-50	18
-17.50	-0.67	-50	9
-15.75	-0.60	-56	6
-14.00	-0.54	-39	3
-12.25	-0.47	-32	3
-10.50	-0.40	-34	5
-8.75	-0.34	-35	7
-7.00	-0.27	-34	9
-5.25	-0.20	-31	9
-3.50	-0.13	-13	5
-1.75	-0.07	-15	4
0.00	0.00	-0	3
1.75	0.07	12	4
3.50	0.13	25	8
7.00	0.27	60	4
8.75	0.34	55	3
12.25	0.47	70	3
HCG 31c			
-21.00	-1.15	23	32

Table 15—Continued

r (arcsec)	r/R_{25}	$V(r)$ (km s ⁻¹)	$dV(r)$ (km s ⁻¹)
-19.25	-1.05	51	5
-17.50	-0.96	18	6
-15.75	-0.86	8	7
-12.25	-0.67	28	17
-8.75	-0.48	27	7
-7.00	-0.38	11	4
-3.50	-0.19	0	1
-1.75	-0.10	-5	1
0.00	0.00	0	0
1.75	0.10	-3	0
3.50	0.19	-8	0
5.25	0.29	-17	1
8.75	0.48	-34	2
10.50	0.57	-34	3
12.25	0.67	-40	5
14.00	0.77	-12	13
15.75	0.86	24	13
HCG 37b			
-24.50	-0.47	163	42
-17.50	-0.34	82	43
-3.50	-0.07	230	51

Table 15—Continued

r (arcsec)	r/R_{25}	$V(r)$ (km s ⁻¹)	$dV(r)$ (km s ⁻¹)
-1.75	-0.03	97	42
0.00	0.00	0	45
1.75	0.03	-139	46
3.50	0.07	-266	55
5.25	0.10	-67	66
HCG 38a			
-14.00	-0.63	181	14
-12.25	-0.55	181	18
-10.50	-0.48	141	17
-8.75	-0.40	131	14
-7.00	-0.32	151	14
-5.25	-0.24	114	19
-3.50	-0.16	123	11
-1.75	-0.08	38	10
0.00	0.00	0	11
1.75	0.08	-68	10
3.50	0.16	-73	13
5.25	0.24	-146	12
8.75	0.40	-147	14
10.50	0.48	-133	11
12.25	0.55	-80	14

Table 15—Continued

r (arcsec)	r/R_{25}	$V(r)$ (km s ⁻¹)	$dV(r)$ (km s ⁻¹)
14.00	0.63	-145	18
HCG 40c			
-22.75	-0.62	186	10
-21.00	-0.57	187	9
-19.25	-0.52	201	8
-17.50	-0.47	189	8
-15.75	-0.43	177	11
-14.00	-0.38	168	11
-10.50	-0.28	177	17
-7.00	-0.19	159	9
-5.25	-0.14	108	9
-3.50	-0.09	102	13
-1.75	-0.05	39	14
0.00	0.00	-0	9
1.75	0.05	-30	10
3.50	0.09	-54	8
5.25	0.14	-105	11
7.00	0.19	-142	10
8.75	0.24	-185	8
10.50	0.28	-202	7
12.25	0.33	-198	7

Table 15—Continued

r (arcsec)	r/R_{25}	$V(r)$ (km s ⁻¹)	$dV(r)$ (km s ⁻¹)
14.00	0.38	-209	9
15.75	0.43	-231	16
17.50	0.47	-236	16
19.25	0.52	-239	16
HCG 44a			
-49.00	-0.49	-196	29
-45.50	-0.45	-95	51
-28.00	-0.28	-274	27
-19.25	-0.19	-66	39
-8.75	-0.09	-143	34
-5.25	-0.05	-181	29
-3.50	-0.03	-168	28
-1.75	-0.02	-65	28
3.50	0.03	208	27
5.25	0.05	242	34
7.00	0.07	196	29
8.75	0.09	271	29
12.25	0.12	388	42
22.75	0.23	233	27
24.50	0.24	222	28
26.25	0.26	220	26

Table 15—Continued

r (arcsec)	r/R_{25}	$V(r)$ (km s ⁻¹)	$dV(r)$ (km s ⁻¹)
28.00	0.28	236	26
29.75	0.30	242	27
31.50	0.31	241	30
HCG 44c			
-38.50	-0.68	-177	15
-36.75	-0.65	-139	9
-35.00	-0.62	-135	10
-33.25	-0.59	-157	16
-31.50	-0.55	-151	14
-29.75	-0.52	-145	14
-28.00	-0.49	-124	29
-5.25	-0.09	-86	24
-3.50	-0.06	-71	9
-1.75	-0.03	-75	4
0.00	0.00	0	3
1.75	0.03	83	5
3.50	0.06	102	6
5.25	0.09	125	12
35.00	0.62	87	29
36.75	0.65	159	20
38.50	0.68	147	22

Table 15—Continued

r (arcsec)	r/R_{25}	$V(r)$ (km s ⁻¹)	$dV(r)$ (km s ⁻¹)
40.25	0.71	177	14
42.00	0.74	164	20
HCG 44d			
-36.75	-0.54	86	18
-35.00	-0.52	95	10
-33.25	-0.49	123	10
-31.50	-0.47	99	10
-29.75	-0.44	97	10
-28.00	-0.41	79	11
-26.25	-0.39	74	14
-24.50	-0.36	76	11
-22.75	-0.34	51	11
-21.00	-0.31	48	14
-19.25	-0.28	34	15
-17.50	-0.26	30	10
-15.75	-0.23	45	10
-14.00	-0.21	48	15
-12.25	-0.18	64	13
-10.50	-0.16	52	12
-8.75	-0.13	44	10
-7.00	-0.10	47	11

Table 15—Continued

r (arcsec)	r/R_{25}	$V(r)$ (km s ⁻¹)	$dV(r)$ (km s ⁻¹)
-5.25	-0.08	39	25
-3.50	-0.05	52	15
-1.75	-0.03	27	22
0.00	0.00	0	13
3.50	0.05	21	20
5.25	0.08	40	14
7.00	0.10	22	11
8.75	0.13	20	11
10.50	0.16	24	12
12.25	0.18	27	9
15.75	0.23	32	10
17.50	0.26	27	12
19.25	0.28	25	10
21.00	0.31	13	10
22.75	0.34	-6	10
24.50	0.36	-23	9
26.25	0.39	-16	9
28.00	0.41	-17	9
29.75	0.44	-19	9
31.50	0.47	-17	11

Table 15—Continued

r (arcsec)	r/R_{25}	$V(r)$ (km s ⁻¹)	$dV(r)$ (km s ⁻¹)
-28.00	-0.41	-174	32
-26.25	-0.39	-159	29
-24.50	-0.36	-158	28
-22.75	-0.34	-128	27
-21.00	-0.31	-116	26
-19.25	-0.28	-121	31
-12.25	-0.18	-219	30
-10.50	-0.16	-213	29
-8.75	-0.13	-178	34
0.00	0.00	0	33
1.75	0.03	60	36
7.00	0.10	143	26
8.75	0.13	166	27
10.50	0.16	171	27
12.25	0.18	154	27
HCG 53a			
-36.75	-0.53	-251	38
-35.00	-0.50	-262	33
-33.25	-0.48	-236	32
-31.50	-0.45	-252	32
-29.75	-0.43	-245	32

Table 15—Continued

r (arcsec)	r/R_{25}	$V(r)$ (km s ⁻¹)	$dV(r)$ (km s ⁻¹)
-28.00	-0.40	-255	32
-26.25	-0.38	-245	32
-24.50	-0.35	-263	34
-22.75	-0.33	-243	33
-21.00	-0.30	-258	33
-19.25	-0.28	-260	33
-17.50	-0.25	-259	33
-15.75	-0.23	-243	32
-14.00	-0.20	-243	32
-12.25	-0.18	-245	33
3.50	0.05	106	41
10.50	0.15	149	43
14.00	0.20	207	34
15.75	0.23	222	32
17.50	0.25	226	32
19.25	0.28	241	33
21.00	0.30	264	32
22.75	0.33	210	34
24.50	0.35	228	33
26.25	0.38	216	37
28.00	0.40	237	33

Table 15—Continued

r (arcsec)	r/R_{25}	$V(r)$ (km s ⁻¹)	$dV(r)$ (km s ⁻¹)
29.75	0.43	212	35
31.50	0.45	211	33
33.25	0.48	248	33
35.00	0.50	226	35
36.75	0.53	272	37
47.25	0.68	278	37
HCG 61c			
-19.25	-0.37	-197	35
-17.50	-0.34	-226	10
-15.75	-0.30	-186	9
-14.00	-0.27	-168	7
-12.25	-0.24	-165	7
-10.50	-0.20	-161	8
-8.75	-0.17	-136	9
-7.00	-0.14	-140	11
-5.25	-0.10	-127	9
-3.50	-0.07	-102	9
-1.75	-0.03	-63	9
0.00	0.00	0	9
1.75	0.03	66	9
3.50	0.07	92	11

Table 15—Continued

r (arcsec)	r/R_{25}	$V(r)$ (km s ⁻¹)	$dV(r)$ (km s ⁻¹)
5.25	0.10	156	17
7.00	0.14	195	18
HCG 68c			
-63.00	-0.82	172	51
-61.25	-0.80	-184	32
-43.75	-0.57	190	18
-42.00	-0.55	188	16
-33.25	-0.43	156	26
-31.50	-0.41	193	23
-29.75	-0.39	209	21
-28.00	-0.37	172	18
-26.25	-0.34	217	23
-5.25	-0.07	228	44
-3.50	-0.05	147	23
-1.75	-0.02	41	8
0.00	0.00	0	6
1.75	0.02	-28	8
3.50	0.05	-81	21
21.00	0.27	-137	16
22.75	0.30	-184	21
24.50	0.32	-162	14

Table 15—Continued

r (arcsec)	r/R_{25}	$V(r)$ (km s ⁻¹)	$dV(r)$ (km s ⁻¹)
26.25	0.34	-156	21
28.00	0.37	-176	20
29.75	0.39	-166	20
31.50	0.41	-161	13
33.25	0.43	-179	15
35.00	0.46	-164	14
36.75	0.48	-180	15
38.50	0.50	-201	21
HCG 71a			
-15.75	-0.50	25	18
-14.00	-0.44	31	14
-12.25	-0.39	17	19
-10.50	-0.33	31	17
-3.50	-0.11	-29	21
-1.75	-0.06	-48	19
0.00	0.00	0	15
1.75	0.06	53	15
3.50	0.11	91	18
5.25	0.17	-5	36
8.75	0.28	174	63
14.00	0.44	36	23

Table 15—Continued

r (arcsec)	r/R_{25}	$V(r)$ (km s ⁻¹)	$dV(r)$ (km s ⁻¹)
15.75	0.50	35	16
17.50	0.56	45	18
22.75	0.72	46	18
26.25	0.83	100	18
HCG 73a			
-22.75	-0.55	93	44
-10.50	-0.25	103	54
-7.00	-0.17	43	29
-5.25	-0.13	19	18
-3.50	-0.08	-2	16
-1.75	-0.04	-7	21
0.00	0.00	0	19
1.75	0.04	-49	25
3.50	0.08	-52	26
5.25	0.13	-53	27
7.00	0.17	-63	28
8.75	0.21	-52	26
10.50	0.25	-70	38
22.75	0.55	-42	26
24.50	0.59	-60	26
26.25	0.63	18	17

Table 15—Continued

r (arcsec)	r/R_{25}	$V(r)$ (km s ⁻¹)	$dV(r)$ (km s ⁻¹)
HCG 79d			
-15.75	-0.56	40	24
-12.25	-0.44	23	15
-10.50	-0.37	48	12
-8.75	-0.31	-7	28
-7.00	-0.25	4	17
-5.25	-0.19	35	13
-3.50	-0.12	14	6
-1.75	-0.06	-4	4
0.00	0.00	0	4
1.75	0.06	-11	5
3.50	0.12	-37	6
5.25	0.19	-39	5
7.00	0.25	-43	3
8.75	0.31	-43	4
12.25	0.44	-80	9
HCG 80a			
-7.00	-0.28	235	15
-5.25	-0.21	167	11
-3.50	-0.14	170	7
-1.75	-0.07	103	7

Table 15—Continued

r (arcsec)	r/R_{25}	$V(r)$ (km s ⁻¹)	$dV(r)$ (km s ⁻¹)
0.00	0.00	0	6
1.75	0.07	-80	6
3.50	0.14	-107	7
5.25	0.21	-72	21
HCG 87a			
-31.50	-0.79	335	29
-29.75	-0.75	310	15
-28.00	-0.70	294	14
-26.25	-0.66	269	16
-24.50	-0.62	265	16
-22.75	-0.57	237	15
-21.00	-0.53	212	14
-19.25	-0.48	204	14
-17.50	-0.44	187	16
-15.75	-0.40	175	15
-14.00	-0.35	151	17
-12.25	-0.31	135	14
-10.50	-0.26	118	16
-8.75	-0.22	84	15
-7.00	-0.18	68	14
-5.25	-0.13	62	15

Table 15—Continued

r (arcsec)	r/R_{25}	$V(r)$ (km s ⁻¹)	$dV(r)$ (km s ⁻¹)
-3.50	-0.09	27	15
-1.75	-0.04	22	16
0.00	0.00	-0	19
5.25	0.13	-111	18
7.00	0.18	-100	21
HCG 87c			
-10.50	-0.49	-228	40
-8.75	-0.41	-166	13
-7.00	-0.33	-137	8
-5.25	-0.25	-110	8
-3.50	-0.16	-92	9
-1.75	-0.08	-57	8
0.00	0.00	0	9
1.75	0.08	39	8
3.50	0.16	75	8
5.25	0.25	97	9
7.00	0.33	127	19
8.75	0.41	94	11
10.50	0.49	89	10
12.25	0.57	99	12
14.00	0.65	125	11

Table 15—Continued

r (arcsec)	r/R_{25}	$V(r)$ (km s ⁻¹)	$dV(r)$ (km s ⁻¹)
15.75	0.74	145	11
HCG 88a			
-21.00	-0.47	254	29
-19.25	-0.43	88	28
-17.50	-0.39	212	28
-15.75	-0.35	213	29
-14.00	-0.31	189	31
-12.25	-0.27	169	29
-10.50	-0.23	172	30
-8.75	-0.19	152	31
-7.00	-0.16	135	31
1.75	0.04	-177	33
3.50	0.08	-215	38
5.25	0.12	-229	33
7.00	0.16	-290	30
8.75	0.19	-304	29
10.50	0.23	-310	29
12.25	0.27	-311	30
14.00	0.31	-318	29
15.75	0.35	-324	32

HCG 88b

Table 15—Continued

r (arcsec)	r/R_{25}	$V(r)$ (km s ⁻¹)	$dV(r)$ (km s ⁻¹)
-21.00	-0.62	49	53
-17.50	-0.51	22	37
-15.75	-0.46	50	24
-12.25	-0.36	62	27
0.00	0.00	0	30
3.50	0.10	-100	46
10.50	0.31	-157	41
12.25	0.36	-177	34
14.00	0.41	-149	31
15.75	0.46	-162	41
17.50	0.51	-166	35
19.25	0.57	-198	36
21.00	0.62	-178	33
22.75	0.67	-175	36
HCG 88c			
-14.00	-0.51	-41	48
-12.25	-0.44	-17	25
-10.50	-0.38	44	34
-8.75	-0.32	-58	27
-7.00	-0.25	11	28
-5.25	-0.19	-27	18

Table 15—Continued

r (arcsec)	r/R_{25}	$V(r)$ (km s ⁻¹)	$dV(r)$ (km s ⁻¹)
-3.50	-0.13	38	25
-1.75	-0.06	27	18
0.00	0.00	0	16
1.75	0.06	21	14
3.50	0.13	26	15
5.25	0.19	62	23
7.00	0.25	78	27
8.75	0.32	122	40
10.50	0.38	150	48
14.00	0.51	109	43
15.75	0.57	135	46
HCG 88d			
-26.25	-0.80	141	5
-24.50	-0.75	139	5
-21.00	-0.64	158	12
-19.25	-0.59	139	6
-17.50	-0.54	146	7
-15.75	-0.48	128	5
-14.00	-0.43	116	6
-12.25	-0.37	109	6
-10.50	-0.32	92	7

Table 15—Continued

r (arcsec)	r/R_{25}	$V(r)$ (km s ⁻¹)	$dV(r)$ (km s ⁻¹)
-8.75	-0.27	107	5
-7.00	-0.21	99	6
-5.25	-0.16	86	6
-3.50	-0.11	65	6
-1.75	-0.05	46	6
0.00	0.00	0	6
1.75	0.05	-25	5
3.50	0.11	-52	5
5.25	0.16	-69	5
7.00	0.21	-66	7
8.75	0.27	-89	5
10.50	0.32	-96	6
12.25	0.37	-93	8
14.00	0.43	-96	13
15.75	0.48	-75	11
17.50	0.54	-96	7
19.25	0.59	-90	8
21.00	0.64	-123	11
HCG 89a			
-17.50	-0.60	159	22
-15.75	-0.54	136	19

Table 15—Continued

r (arcsec)	r/R_{25}	$V(r)$ (km s ⁻¹)	$dV(r)$ (km s ⁻¹)
-14.00	-0.48	110	18
-12.25	-0.42	114	18
-10.50	-0.36	75	19
-5.25	-0.18	142	24
-3.50	-0.12	127	20
-1.75	-0.06	49	15
0.00	0.00	0	14
1.75	0.06	-92	17
3.50	0.12	-121	19
5.25	0.18	-148	22
7.00	0.24	-153	24
8.75	0.30	-125	26
15.75	0.54	-131	23
17.50	0.60	-152	22
19.25	0.66	-152	21
21.00	0.72	-143	20
22.75	0.78	-146	22
HCG 92a			
-43.75	-0.63	-128	28
-42.00	-0.60	-136	24
-28.00	-0.40	-77	33

Table 15—Continued

r (arcsec)	r/R_{25}	$V(r)$ (km s ⁻¹)	$dV(r)$ (km s ⁻¹)
-24.50	-0.35	-121	29
-22.75	-0.33	-90	26
-21.00	-0.30	-104	24
-19.25	-0.28	-107	23
-17.50	-0.25	-117	23
-10.50	-0.15	-100	28
-7.00	-0.10	-62	27
-5.25	-0.08	-47	25
-3.50	-0.05	-47	25
-1.75	-0.03	-45	26
3.50	0.05	-7	24
5.25	0.08	11	24
7.00	0.10	-13	29
8.75	0.13	28	24
10.50	0.15	48	31
15.75	0.23	19	27
17.50	0.25	35	28
19.25	0.28	37	23
21.00	0.30	45	24
22.75	0.33	57	24
24.50	0.35	89	25

Table 15—Continued

r (arcsec)	r/R_{25}	$V(r)$ (km s ⁻¹)	$dV(r)$ (km s ⁻¹)
26.25	0.38	58	24
28.00	0.40	55	23
29.75	0.43	40	23
31.50	0.45	34	23
33.25	0.48	42	23
35.00	0.50	46	23
36.75	0.53	26	25
HCG 92c			
-7.00	-0.13	-320	42
-5.25	-0.10	-259	41
-3.50	-0.07	-142	19
-1.75	-0.03	-17	7
0.00	0.00	0	7
1.75	0.03	-36	9
3.50	0.07	-127	26
19.25	0.36	-178	45
HCG 93b			
-14.00	-0.24	91	10
-12.25	-0.21	93	4
-10.50	-0.18	25	6
-8.75	-0.15	8	4

Table 15—Continued

r (arcsec)	r/R_{25}	$V(r)$ (km s ⁻¹)	$dV(r)$ (km s ⁻¹)
-7.00	-0.12	7	4
-5.25	-0.09	-28	4
-3.50	-0.06	7	7
-1.75	-0.03	34	4
0.00	0.00	-0	5
1.75	0.03	-83	10
5.25	0.09	-23	29
7.00	0.12	-97	16
8.75	0.15	-92	4
10.50	0.18	-119	4
12.25	0.21	-162	4
14.00	0.24	-198	4
15.75	0.27	-195	4
17.50	0.30	-214	9
19.25	0.34	-217	19
HCG 93c			
-10.50	-0.29	154	50
-5.25	-0.15	111	36
-1.75	-0.05	33	41
1.75	0.05	-152	44
3.50	0.10	-266	42

Table 15—Continued

r (arcsec)	r/R_{25}	$V(r)$ (km s ⁻¹)	$dV(r)$ (km s ⁻¹)
5.25	0.15	-298	39
17.50	0.49	-339	38
HCG 96a			
-3.50	-0.11	-276	151
-1.75	-0.05	-23	38
0.00	0.00	0	29
1.75	0.05	66	46
3.50	0.11	84	50
5.25	0.16	96	62
7.00	0.21	94	53
10.50	0.32	130	74